

Contents

1	INTRODUCTION	5
2	MULTI-PURPOSE CHAOTIC PENDULUM	8
2.1	Introduction	8
2.2	Background	8
2.3	Theoretical Considerations	8
2.4	Experimental Results	9
2.5	Hysteresis and Amplitude Jumps	10
3	APPARATUS	12
3.1	Drive System	12
3.2	Sensor	12
3.3	Drive Amplitude Control	13
3.4	Friction	13
3.5	SDC Sensors	13
3.6	Lock-in Amplifier	15
3.7	Electronics	21
4	The Computerized Pendulum	24
4.1	General	24
4.2	Algorithms	24
4.3	Phase Space	27
4.4	Poincare' Sections	30
5	PETERS AUTOMATED PENDULA (PAPA)	35
5.1	Precision Simple Pendulum	35
5.2	Conical Pendulum	36
5.3	Adjustable Trends Pendulum	37
5.4	Kalman Filtered Pendulum	38
5.5	Support Constrained Pendulum	39
5.6	Ink-jet Pendulum	40
5.7	Cavendish Balance (Pendulum)	40
5.8	Long Period Pendulum	41
5.9	Tilt Sensitive Pendulum	42
5.10	Modified Analytic Balance (Pendulum)	43
5.11	Leaky Pendulum	43
5.12	Torsion Gravity Pendulum	45
5.13	Multi-Purpose Chaotic Pendulum	45
5.14	Servo Controlled Balance (Pendulum)	46

List of Figures

1	Resonance curve for the weakly driven pendulum.	9
2	Large asymmetry and hysteresis when the drive is moderate.	10
3	Illustration of the velocity sensor.	13
4	Block Diagram of the SDC Electronics connected to a sensor.	14
5	Block diagram of a Lock-in Amplifier.	15
6	Operations performed by the synchronous detector.	15
7	SDC Planar Geometry Position Sensor.	18
8	Equivalent circuit of the SDC Sensor.	18
9	An array for measuring linear position. (The electrodes are shown separated for clarity.)	19
10	An array for measuring angular position. (Electrodes shown separated for clarity.) . . .	20

11	Illustration of an array for unlimited range measurement.	21
12	Electronics used in the Multi-Purpose Chaotic Pendulum.	22
13	Example output from program (3) of the Pendulum Simulations Menu.	25
14	Example output from the pendulum—both graphs for a period-1 limit cycle.	27
15	Example software generated Phase Space trajectories of the pendulum.	28
16	Example output from the pendulum—a chaotic phase space plot.	29
17	Example chaotic time records generated by the pendulum.	29
18	Pendulum generated graphs—period-5 limit cycle.	29
19	Poincare' sections corresponding to chaos.	30
20	Simulated Poincare' section (standard) corresponding to chaos.	31
21	Power spectra using HIM program (5), followed by GSM program #26.	31
22	Order of calculations in the Fourier Transform.	32
23	Simulation of the bell ringer pendulum mode using PSM pgm. #6.	33
24	Example simple pendulum suitable for automation.	36
25	Motion of a Conical Pendulum.	36
26	Support Constrained Rigid Spherical Pendulum.	39
27	Cavendish Balance outfitted with two SDC sensors.	40
28	Long Period Pendulum for Mesodynamic Studies.	41
29	Tilt Sensitive Pendulum.	42
30	Modified Analytic Balance Pendulum.	43
31	Illustration of the Leaky Pendulum.	44
32	Torsion-Gravity Pendulum.	45
33	Illustration of an LRDC Transducer.	46
34	Block Diagram of a servo-controlled pendulum.	47

PREFACE

The Multi-Purpose Chaotic Pendulum and other instruments either offered or being contemplated for development by TEL-Atomic Inc, are a versatile mix of both the oldest and newest training tools. Using the symmetric differential capacitive (SDC) sensors, these novel instruments offer brand new opportunities in education. They're even responsible for pioneering research in an old area— anelasticity. In all cases they are mechanical oscillators, labeled generically by the term, pendulum. The pendulum has become the paradigm of nonlinear physics; and most students unabashedly love it. Through computer automation, the pendula described herein provide a fresh approach to the study of classical mechanics, as well as equipping the student with some tools for the study of chaos that were not previously available.

Although the instruments which have been commercialized are excellent for physics education, their optimum utilization requires documentation that has not existed. Thus it was decided that I would write a monograph on mechanical system dynamics to be provided with the operating manual for certain instruments. A significant portion of this monograph involves material that cannot be found in its present form anywhere else. It derives from research performed at Texas Tech University since 1986, attempting to understand processes in an area that wasn't readily accessible before the invention of the SDC sensors. The physics of this work has been labeled "mesodynamic complexity in mechanical systems". Some features of this work are simple enough for an introductory student to understand, whereas others are presently without explanation. Relative to the latter, a fundamental excitation called the "krazon" has been postulated. This excitation is envisioned as being to the defect lattice structures of the anelastic world of metals (involving stress-strain hysteresis) what phonons are to the ideal lattice. Being wavelike, they are the carriers of energy for irreversible deformation; i.e., the vehicle for converting macro-strains into heat (internal friction). Moreover, following the lead of Dr. Thomas Erber of Illinois Tech University, a dissipative counterpart to quantized flux jumps has been predicted, called the "hysteron". The present monograph does not go into great detail concerning the basis for these predictions; however, for the one who is interested in knowing more, there are references to scientific papers which have been published. On the other hand, some discoveries which are reasonably easy to understand; such as the bell-ringer mode of the conventional pendulum, are herein described.

Since chaos is impacting such a large number of disciplines, it was determined that classical material dealing with nonlinear systems other than the pendulum would also be included in the monograph. One goal of this project has been that all of the topics be presented in as simple a form as possible. For example, the Cromer-Euler algorithm permits the integration routines of many systems to be dealt with in a more intuitive (while still computationally acceptable) manner than other schemes, such as Runge Kutta.

Inherent to the new science of chaos and complexity is a new philosophy—one that requires an unconventional way of thinking about physics. Ironically, the approach to physics which is most effective in this work is "the old school" type; one that refuses to focus exclusively on a single topic. This is because the very nature of the new science is inconsistent with what has become conventional in physics—reductionism, or convergent thinking. In general, divergent thinking has a greater probability for creativity.

Since joining Texas Tech University I've researched 14 different forms of the oldest instrument of experimental physics, the pendulum. This monograph describes all of these pendula, some of which are currently available as commercial products from TEL Atomic Inc. The computer programs which are a part of this package were developed for a special topics course (Physics 5300—Chaos and Complexity) which I taught in the spring of 1994.

I'm proud to be an instrumentalist and have aspired to the excellence demonstrated by those who in times past dramatically changed the course of modern physics by their hands on broad experience in the development of experimental apparatus. It is hoped that those who identify with this spirit will be enthusiastic about these new instruments.

The endorsement of my work by TEL-Atomic, Inc. has truly been a blessing. Steve Starling saw promise in my sensors even in the early stages of development. Along with others, Steve's wife, Sharon, has helped me view the comments by some colleagues from a healthier perspective. The Starling's support has been refreshing, and I thank them.

This work would not have been possible without significant help from some really outstanding peo-

ple; help that started with my father, mother and older brother Palmer—gently assisting my steps. I only wish that my father, who introduced me to the Lord, were still here. My wife, Rosalee, deserves highest praise for her unwavering support. Our daughters Heather, Leslie, and Emily; and our son, Benjamin—have supplied all the encouragement we could want for. Their faithfulness is reflected in the next generation—granddaughters Caitlin, Bethany, and Lauren. My pastor Delmar Ross, of Trinity Church, has provided continual spiritual encouragement. His decades of devotion to Jesus Christ has been a model for all to follow. His practical counsel is a significant reason for our family being blessed. On more natural, as opposed to spiritual matters, I've had a gracious and talented teacher of computerized (compiled) typesetting, in the person of physics graduate student, Brian McCuistian. For what they've sown into this work, I pray that God will bless each of these individuals abundantly.

Randall D. Peters
Lubbock, Texas (1995)

Cover: This pattern was generated with the ink-jet version of the support constrained pendulum described on p. 40.

1 INTRODUCTION

Physics was at a point of juncture in the early part of the 20th century. It could vigorously pursue those phenomena which yield themselves to the now conventional reductionist approach; or it could pursue the business of many body systems, in which a different kind of thinking is necessary. Of course our history has been that of the the path that was followed—reductionism . Before the close of the 20th century, it appears that our focus will increasingly turn away from reductionism and towards synergetics. In the 1920's it was not possible to be effective in the field of complexity (involving many body synergetics) because the computer had not yet been invented. With the advent of the personal computer and its distribution to the hands of many investigators, we may be poised to attack some fundamental but forgotten physics. For example, what is the cause for the Portevin LeChatelier (PLC) effect, a many body cooperative phenomenon) that was published in 1923, hardly noticed, and since then mainly forgotten. Why would an important process such as this be treated the way it was? Maybe we'll never know for sure; fortunately there are some efforts to revive interest, such as G. Venkataraman's Fermi Conference monograph [1]. Although he admonished physicists in the 1960's to get involved in this area, which he felt should become an important new field, it still remains mostly unnoticed. Historically, science has experienced revolutions every century or so. Toward the end of the 19th century there were those who thought that the only thing which remained of our science was "tying up loose ends" of classical physics. Now there are those at the end of the 20th century who hold a similar view, except that the loose ends involve "modern physics". The "fly in this ointment" however, may be chaos and complexity. If we're to be properly equipped for this discipline, we must broaden our expertise from narrow fields of study. Support for this statement can be found in an article in Scientific American by Nobel Laureate Philip W. Anderson [2]. There, it is said of Anderson: "He is a potent proselytizer, writing with lyrical fervor on how the interplay of order and disorder found in condensed matter systems can serve as a metaphor for life itself". Anderson also "began challenging the hegemony of particle physics and of the entire reductionist paradigm of modern science long before it became fashionable to do so". He pointed out that by the late 1960's "the particle physicists were claiming on all sides that they were doing *the* fundamental science, and what the rest of us were doing was just engineering." He challenged this contention in his "More is Different" article, pointing out that "reality has a hierarchical structure, with each level independent, to some degree, of the levels above and below. At each stage entirely new laws, concepts, and generalizations are necessary, requiring inspiration and creativity to as great a degree as in the previous one. Thus, for example, psychology is not applied biology, nor is biology applied chemistry." Perhaps the most quotable quote of all is his closing statement: "When one understands everything, one has gone crazy!".

What we call modern physics ceased to be properly labeled by the term with the discovery of chaos and complexity. One individual was quoted in the book by Gleick [3] as saying that the 20th century will be remembered for 3 things: relativity, quantum mechanics, and chaos (including complexity). Not everyone agrees with the inclusion of the 3rd item in this prediction. This should come as no surprise, since chaos was observed for years but steadfastly claimed to be environmental noise rather than recognized for what it is—intrinsic to the system being studied. Even well known champions of nonlinearity (in classical form) have not necessarily embraced this new field. A case in point was Hayashi's unwillingness to recognize the seminal work of his student Ueda [4]. It took Ueda nearly 20 years to publish his discoveries.

When it comes to the properties of metals, pragmatists have known for years that defect structures regulate many of their physical properties. Perhaps this is not surprising to a solid state physicist trained in semiconductors. Were it not for defects, the whole of the information age, borne of the transistor, would be impossible. Whereas the physics of defects in semiconductors has been studied passionately on every front, defects of metals as a subject for study has been mostly ignored by physicists, although some of the greatest scientists of all time were intrigued with the subject at the end of the 19th century. Additionally, it was a subject of considerable interest to Richard Feynman.

Some physicists recognize as "fundamental" only studies that involve reductionism. Nevertheless, synergy in a many body system can cause the whole to be greater than the sum of its parts taken individually. In the case of complex systems, this means that there are properties that will never be explained by physics theory as it is currently known and practiced. Failure to recognize such properties

as fundamental is, in effect, to deny their existence. A perfect example of this was the rejection of Maiman's paper on the ruby laser by *Physical Review Letters*. As Bardeen has pointed out [5], the laser is a macroscopic quantum system. Unlike conventional light sources in which the atoms practice Frank Sinatra's theme song "I did it my way", atoms in a laser are involved in synergetics. Mesoanelastic complexity is also an example of atoms involved in synergetics. However, until better instrumentation was available (such as the SDC transducers), work in this field was hampered.

Instrumentation is at the very heart of significant advances in physics. For example, physics as we know it was largely birthed by Galileo's turning the telescope to the cosmos. He recognized the following truth: "Improve a measurement by a factor of 2 or 3 and you'll see new physics; improve it an order of magnitude and you may change the history of physics".

Interest in chaos and complexity is probably increasing at an exponential rate, as evidenced by publications on the subject. The following observations are largely excerpts which were taken from *Physics Today* articles that have appeared over the last several years.

First of all, it should be recognized that what we call modern physics should really now be labeled "postmodern" [6]. Second, chaos and complexity are an interdisciplinary subject with which physicists, in part because of the trend toward specialization rather than generalization, are mostly inexperienced. Many outstanding physicists, however, have increasingly departed from the trend, as evidenced by a quote by Philip Anderson: "Almost without exception, the more eminent, the more deeply committed, the more successful within a given field a scientist is, the more eager that scientist is to relate to scholars outside his or her field.....[7]"

In his article, "A lesson in humility" [8] Dan Kleppner says: "Given that physicists generally esteem simplicity, it is remarkable that the study of complexity has moved to center stage, but such are the ironies of nature". "Its central theme—the elaboration of forms from the repetition of simple operations—is being recognized as a fundamental organizing principle of nature". "Only in the past few years, however, have nonlinear dynamics and chaos theory entered the mainstream of physics. The last physics survey hardly noticed that classical mechanics was on the threshold of a renaissance."

James Gleick has provided a good overview of the subject in his book. In polling numerous experts he has capsulized many qualitative features, such as (p.43): "Those studying chaotic dynamics discovered that the disorderly behaviour of simple systems acted as a creative process. It generated complexity; richly organized patterns, sometimes stable and sometimes unstable, sometimes finite and sometimes infinite, but always with the fascination of living things." Gleick has included a quote of particular significance to the present work. A young physicist asked Stephen Smale (U. Calif. Berkeley) what he was working on. The answer stunned him: "Oscillators." It was absurd. Oscillators—pendulums, spring, or electrical circuits—were the sort of problem that a physicist finished off early in his training. They were easy. Why would a great mathematician be studying elementary physics? Not until years later did the young man realize that Smale was looking at nonlinear oscillators, chaotic oscillators, and seeing things that physicists had learned not to see.

Time will tell if the 20th century will be noted for chaos and complexity as well as relativity and quantum mechanics. One piece in the picture is that the 1991 Nobel prize to Pierre-Gilles de Gennes is for work on complex systems. His work was with liquid crystal polymers "that, from the outside, looked very complicated, with a literature that was incomprehensible to virtually all physicists, .. he figured out how to think about them simply. He knew the right questions to ask: What is the order parameter for this system? What are its symmetries? What are its broken symmetries? "A large number of experiments followed naturally from that approach" [9]. His philosophy has been one of recognizing ... the benefits from cross-fertilization among physicists, chemists and materials scientists". He is quoted as saying that "...over the last ten years, his thinking has been less in terms of complex mathematics and more in terms of scaling laws" (one of the hallmarks of complexity).

References

- [1] G. Venkataraman, *Proc. Fermi Int. Sch. Phys. LXXXII*, Caglioti & Milone eds., pp 278-414 (1982).
- [2] Philip W. Anderson, *Scientific American*, p. 34, Nov. 1994.

- [3] J. Gleick, *Chaos, Making a New Science*, Viking, New York, 1987.
- [4] F. Moon, *Chaotic and Fractal Dynamics, An Introduction for Applied Scientists and Engineers*, Wiley, New York, 1992 (see page 149 for the discussion concerning Ueda).
- [5] J. Bardeen, *Physics Today* 43 (12), 25 (1990).
- [6] Heller & Tomsovic, "Postmodern quantum mechanics", July 1993, *Phys. Today*.
- [7] *Physics Today*, June, 1992.
- [8] *Physics Today*, Dec. 1991.
- [9] *Physics Today*, Dec. 1991, p. 17.

2 MULTI-PURPOSE CHAOTIC PENDULUM

2.1 Introduction

The simple harmonic oscillator (SHO) is of fundamental importance to linear systems, whereas the pendulum has become the paradigm of nonlinear physics. Nearly isochronous at low levels of motion, the pendulum has been the mainstay of elementary analysis for hundreds of years. Additionally, its period increase at large amplitudes has been part of the core material for upper level undergraduate courses in mechanics¹. Even before the discovery of its chaotic properties, the pendulum had become one of the classic nonlinear systems, along with a small number of other cases such as the Duffing oscillator²⁻⁴. After numerous studies, the importance of the pendulum to nonlinear work has become generally recognized. The person most responsible for this is Chirikov⁵.

One should probably beware of the term “simple” in the description of any physical system. For example, in spite of the popularity of the pendulum; one of its properties that may not have been previously reported was recently discovered (R. Peters, “Resonance response of a moderately driven rigid planar pendulum”, to be published in the American Journal of Physics, 1995). It is a property that is not counter-intuitive; however, an apparatus development effort was necessary for it to be noticed. It is a property that has nothing to do with chaos and strange attractors, but rather with the amplitude of steady state motion as the pendulum is tuned through resonance. The drive amplitudes employed are small enough that the motion is restricted to period-one limit cycles at steady state. The bifurcation route to chaos is thus not allowed. Practically, this amounts to $\theta < \pi$ always.

2.2 Background

It is recommended that the resonance response of a damped SHO (c.f. [1]) be reviewed for a better understanding of the material in this monograph. For the SHO, the change in both amplitude and phase as the drive frequency is altered is very well known, at least in the limit of steady state motion. The half width of the response is determined by the quality factor (Q) of the oscillator, which is related to the log decrement, determined from free decay.

Although the direction of approach toward resonance (from above or below) is unimportant to the SHO, it can be very important for nonlinear systems. Differences according to direction can give rise to hysteresis in which there are jumps in amplitude. These have been well documented in the case of the van der Pol and Duffing oscillators; however, the resonance response of the pendulum has been almost unstudied.

2.3 Theoretical Considerations

For the most meaningful comparisons of your pendulum with the TEL-Atomic computer simulations, it will be necessary for you to perform the exercises indicated in the section titled “The Computerized Pendulum” (section 4).

The velocity sensor of the apparatus provides a constant damping torque, per unit angular velocity. For the prototype pendulum, this was measured to be $c = 1.9 \times 10^{-4} \text{ kg m}^2/\text{s}$. Marion discusses the log decrement for underdamped motion of the SHO on page 108¹. It is given by $\beta\tau_1$ where $\tau_1 = 2\pi/\omega_1$ and $\omega_1 = (\omega_0^2 - \beta^2)^{\frac{1}{2}}$, which for small damping equals ω_0 . For small amplitudes of the pendulum, the motion becomes that of the SHO and for the present case, $\beta = c/(2I)$, where the moment of inertia, I , of the pendulum comprises three parts. For the prototype these were measured to be (a) $I_0 = 2.8 \times 10^{-5} \text{ kg m}^2$ of the rotating member of the motor, (b) ML^2 of the bob, and (c) $\frac{1}{3}\mu\lambda^2$ of the rod which is clamped to the shaft of the motor at one end. It can be readily shown that $\beta\tau = 2\pi\beta/\omega_0 \approx c\pi\omega_0^3/(Mg^2)$ in the limit that $\frac{1}{2}\mu\lambda \ll ML$ and $ML^2 \gg I_0$. The near proportionality at low levels to the cube of the natural frequency provides a convenient means for adjusting the damping—one simply alters the natural period of the pendulum. This is of considerable pedagogical value in studying conventional linear physics with the pendulum.

Without drive, the equation of motion for the pendulum is

$$I\ddot{\theta} + c\dot{\theta} + g(ML + \frac{1}{2}\mu\lambda)\sin\theta = 0 \quad (1)$$

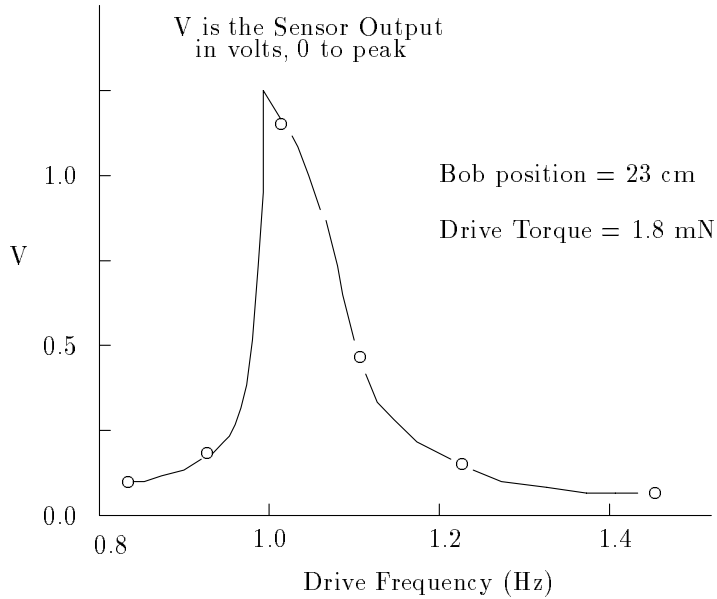


Figure 1: Resonance curve for the weakly driven pendulum.

where, for the prototype, $M = 22 \text{ g}$ is the mass of the bob, adjustable in distance L from the axis on a rod of length $\lambda = 30 \text{ cm}$ and mass $\mu = 14 \text{ g}$. Two different bob positions were considered: (i) $L = 12.5 \text{ cm} \rightarrow 7.92 \times 10^{-4} \text{ kg m}^2$ (total moment) and (ii) $L = 23.0 \text{ cm} \rightarrow 1.61 \times 10^{-3} \text{ kg m}^2$. The measured natural frequency for these two cases was 1.25 Hz and 1.06 Hz respectively. The log decrement, which is given by

$$\beta\tau \approx c\pi / \sqrt{I g (ML + \frac{1}{2}\mu\lambda)} \quad (2)$$

has the value $\beta\tau = 0.10$ and 0.057 for the two cases indicated. (During characterization, one actually goes the other direction; i.e., one measures at least two log-decrements, from which c and I are determined.)

2.4 Experimental Results

With a drive torque of 1.8 mN (peak value, plus or minus), the amplitude was found never to exceed 1.25 rad peak to peak steady state oscillation. For the bob at the 12.5 cm position, the peak in the response was found to occur at 1.2 Hz , barely less than the small amplitude measured 1.25 Hz . A sweep through resonance was performed for each of the two bob positions, 12.5 cm and 23.0 cm . Rather than smoothly varying the frequency (drive fixed at 1.8 mN) the system was switched (different values of the resistor pair on the 555 timer) through the following values: $0.83, 0.92, 1.02, 1.10, 1.20, 1.45, 1.61,$ and 2.08 Hz . Because the step sizes in the drive frequency are large, it was not possible at the 1.8 mN drive level to directly see hysteresis effects. When superposed on a matched theoretical response, however; the introduction of asymmetry due to nonlinearity was evident. In particular, as shown in Fig. 1, there is an obvious “softening” as compared to the SHO. The theoretical curve is from a QuickBasic code which utilizes the Cromer-Euler algorithm⁶; it is provided in Table I of section 4.

In relating simulation output (in rad) to the sensor output (in Volts), the conversion used (case specific) was 1 V/rad , corresponding to the sensor calibration constant (fixed) of 0.15 V per rad/s . Physicists are accustomed to obtaining the angular velocity of oscillation from the product of drive frequency and amplitude. This well known relationship for the SHO is only approximately true for this nonlinear case.

The resonance asymmetry evident in Fig. 1 was not surprising, and has been mentioned in the literature⁷; there also, the drive level was low. At larger drive levels, such as in Fig. 2, things become

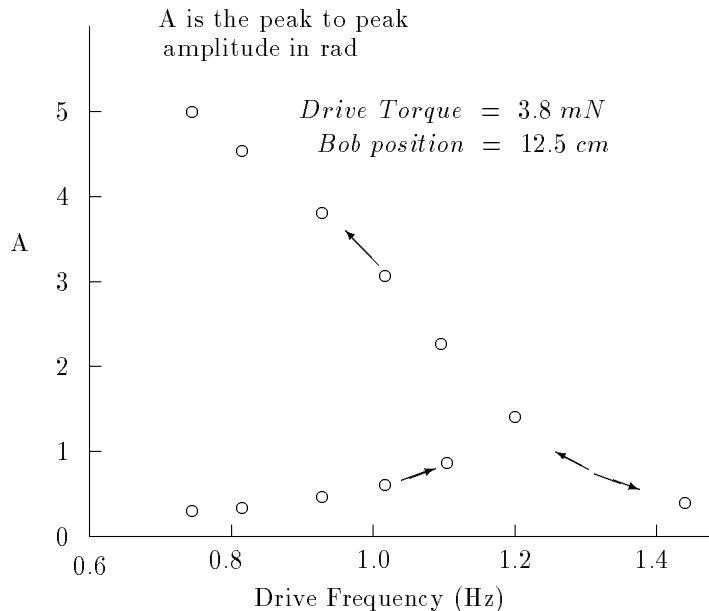


Figure 2: Large asymmetry and hysteresis when the drive is moderate.

much more interesting. Here the drive has been increased to $\pm 3.8 \text{ mN}$.

2.5 Hysteresis and Amplitude Jumps

It can be seen from Fig. 2 that there is a dramatic difference in response according to whether Δf of the frequency change is positive or negative. The very large oscillations at steady state (5 rad peak to peak) are most readily obtained by starting at a frequency above the low level natural resonance frequency and tuning downward.

If the drive torque is increased from 3.8 mN to 5.4 mN, then the maximum allowed value of the peak to peak amplitude of the upper branch is reduced. This happens because the drive is then sufficiently great to cause the bob to “go past vertical”. There is a strong phase perturbation which results, that causes the pendulum to inevitably settle into an amplitude corresponding to the lower branch.

The data plotted are for steady state only. When a downward jump occurs, there is a time interval of transient motion that is quite variable and which can be chaotic (if stimulated by an increase in drive torque—too small for sustained chaotic motion). The number of vertical passages during the transient chaos is extremely variable; we’ve seen everything between 1 and 60. The case for transient chaos is based on the following observation. During each jump, points were collected on the monitor using the Poincare’ section algorithm—based on the embedding theorem. An accumulation of about a dozen individual cases were all different and appear to yield a corporate fractal, or strange attractor.

The upper branch motion is fascinating, even though it is not chaotic. In this branch, large oscillation can be maintained with low drive torques because of the manner in which the period of the pendulum increases with amplitude. To maintain the motion, the phase relation between the pendulum and the drive source is critical. Apparently the limiting case, if it could be realized; is one for which the peak to peak amplitude of 2π occurs at a frequency of zero. In practice, the system’s sensitive dependence on initial conditions makes it very difficult to attain motions much greater than about 5 rad.

The upper branch can be reached by releasing the pendulum from rest at a large displacement at just the right time in the drive cycle. More dependable, however, is to start at a drive frequency above the low level resonance frequency of the pendulum and switch to ever lower values. After each switch, one must wait for transients to settle. The wait becomes increasingly important at the largest amplitudes of the motion, lest the bob “go past vertical” and settle into the lower branch. The time required for transients to settle can be quite long when the damping is small. In one case with an early prototype

pendulum, the Q was sufficiently great that 25 to 30 cycles were required for root sum square changes in the amplitude to drop below about 3%.

The large amplitude periodic motion has come to be labeled the “bell-ringer” mode of the pendulum. When the first prototype of the instrument was exhibited at the national AAPT meeting at Notre Dame in 1994, an Englishman in attendance pointed out that the bell ringers of Europe have used such a motion for many years. In “ringing-up the bell”, the time interval between “dongs” increases as the amplitude is built up. Because so many physicists are musically inclined, it is surprising that this mode would go untreated for so long.

BIBLIOGRAPHY

1. J. Marion and S. Thornton, **Classical Dynamics of Particles and Systems**, 3rd ed., Harcourt Brace Jovanovich, San Diego (1988).
2. P. Hagedorn, **Non-linear Oscillations**, 2nd ed., Clarendon Press, Oxford England (1988).
3. P. Berge, Y. Pomeau, and C. Vidal, **Order within Chaos, Towards a deterministic approach to turbulence**, Wiley, New York (1984).
4. C. Hayashi, **Nonlinear Oscillations in Physical Systems**, Princeton University Press, New Jersey (1964).
5. D. Sahn, S. McWhorter, and T. Uzer, “Generalizing the Chirikov paradigm: a geometrical view”, *J. Chem. Phys.* **91** (1), 219-225 (1989).
6. A. Cromer, “Stable solutions using the Euler algorithm”, *Am. J. Phys.* **49**(5), 455-457 (1981).
7. F. Irons, “Concerning the non-linear behaviour of the forced spherical pendulum including the dowsing pendulum”, *Eur. J. Phys.* **11**, 107-115 (1990).

3 APPARATUS

3.1 Drive System

One of the biggest challenges in studying the pendulum experimentally (or any chaotic mechanical system) involves the drive. The application of a force to properly overcome friction in the system is not trivial. The drive must replace energy lost to friction, but it should not alter the equations of motion other than changing them from homogeneous to inhomogeneous form. The TEL-Atomic apparatus addresses this problem by means of an alternating current (60 Hz) induction motor with small bearing friction. Thus the drive is a torque applied about the axis of the pendulum, which is the armature shaft of the motor. A direct current motor for the apparatus was not considered because of the large amount of commutator friction in such motors.

An induction motor works on the basis of what is effectively a rotating magnetic field (provoking memories of the magnetic suspension work of the late Jesse Beams at the University of Virginia). This rotating field is generated by a minimum of two coils in which a phase difference is introduced, such as with a capacitor in series with one of the windings. As the field rotates, the armature attempts to follow, resulting in a torque. To reverse the direction of the torque, the capacitor is simply switched from one winding to the other. A simple way to do this is to use a double pole double throw (DPDT) relay.

The motor selected for the TEL-Atomic pendulum was not designed for applications involving high torque and power; however, the very first prototype of the apparatus was one which used an ordinary ceiling fan. The torque is of essentially constant magnitude, independent of armature position. Frequency control —time between periodic opening and closing of the DPDT relay, is managed by a 555 timer. The timer's duty cycle was chosen at 50% , thus constituting a square wave. Because the timer is not by itself able to deliver much current, a small transistor (PN2222) was added, in a common emitter configuration, to be driven by the timer and in turn to close the relay. The otherwise large voltage spikes associated with opening of the relay are removed with a diode placed across the relay coil.

Most of the previous work that has been done on the pendulum, particularly in simulation, has used a sinusoidal drive. There are some differences in the response of a pendulum to sine and square wave drives, particularly at low frequencies; but they can be readily studied through the computer simulations provided with this document. The essential features have been found to be nearly equivalent; which is good, because it is much harder to build a suitable sine drive for the pendulum. Moreover, the presence of higher (odd) harmonics in the square wave drive is pedagogically useful.

3.2 Sensor

The TEL-Atomic apparatus uses a velocity sensor for determining all aspects of the pendulum's motion. Position is obtained from the angular velocity using an operational amplifier integrator. The velocity is measured by means of an eddy current sensor. Two small powerful rare earth permanent magnets are located on opposite sides of an aluminum disk mounted on the shaft of the motor as shown in Fig. 3.

As the disk rotates, the magnets tend to be "dragged along" because of the induced eddy currents. The magnets are located on the end of a beryllium-copper cantilever, and the bending of the cantilever is sensed with a symmetric differential capacitance (SDC) sensor. The SDC sensors are a new technology with improved sensitivity and dynamic range as compared to earlier capacitive sensors. In all cases they are full-bridge devices possessing greater symmetry than older differential capacitive (half-bridge) types or single component (quarter-bridge) types. The greater symmetry results in improved immunity to changes in environmental stray capacitance. By using them in an ac bridge, the great advantages of synchronous detection (the heart of a lock-in amplifier) can be exploited. The output from the electronics is a dc voltage which can be monitored in a variety of ways; but for many purposes, such as producing Poincare' sections, a computer is essential. The analog to digital (A to D) converter for the pendulum apparatus need not be sophisticated. The number of bits is not critical (if > 8 bits) since the pendulum motions of interest are for this work quite large. On the other hand, the SDC sensors have been used in a number of other applications where the motions involved are very small, and in those cases a 12 bit A to D converter is desirable to avoid significant rounding errors. The speed of

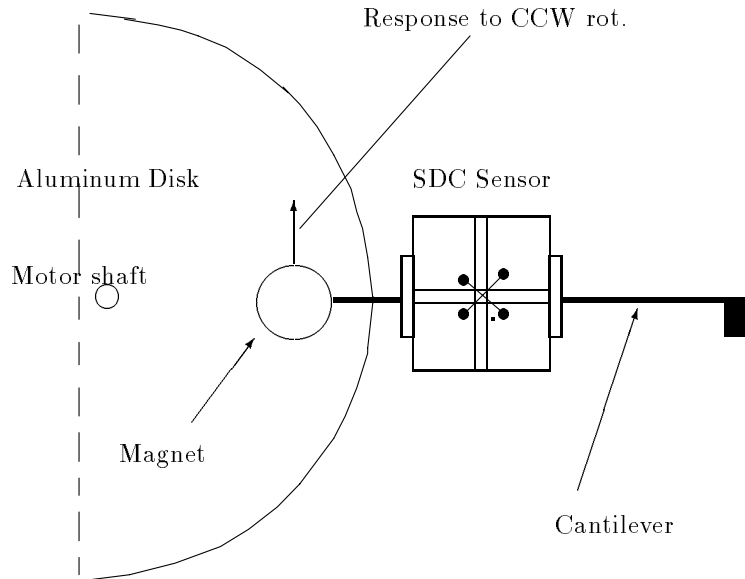


Figure 3: Illustration of the velocity sensor.

the converter also need not be great, since the frequencies of interest are quite low. A serial unit with about 50 bits per second transfer rate is adequate, even though the prototype work was conducted with a Metrabyte Das1401 (and 1601).

3.3 Drive Amplitude Control

The most elegant way to control the drive amplitude would be to use a saturable core reactor, resulting in insignificant Joule heating losses. The power required of the motor, however, is sufficiently low as to make this unnecessary; which is good, because commercial equipment of the indicated type is no longer readily available as in the past. (One might be tempted to use SCR and related devices for control, but pulsed devices do not work well with ac inductive loads.) Thus the amplitude of the drive is determined by how much resistance is placed in series with the motor windings. A convenient way to provide almost continuous control is by using a rheostat with a great enough power rating to accommodate the heat that is generated in this non-ideal but satisfactory method of control.

3.4 Friction

The greatest single source of friction in the Multi-Purpose Chaotic Pendulum, which is supplied by design, is that which derives from eddy currents of the velocity sensor. These currents provide an essentially constant torque per unit angular velocity, which is very convenient. One can readily show from the equation of motion that this provides for a simple means to adjust the damping. Alteration of the moment of inertia of the pendulum gives rise to a different log-decrement of the motion. If the mass of the rod were ignorable compared to that of the bob, then the log-decrement would be proportional to the cube of the natural frequency of the pendulum. Thus one can alter the damping by simply raising or lowering the bob relative to the axis of rotation. Even with non-ignorable rod mass the cubic relationship is close to being obeyed.

3.5 SDC Sensors

A tutorial on SDC sensors is here provided, particularly as relates to the TEL-Atomic MPCP. For the interested reader, the bibliography provides references to other systems in which the SDC technology

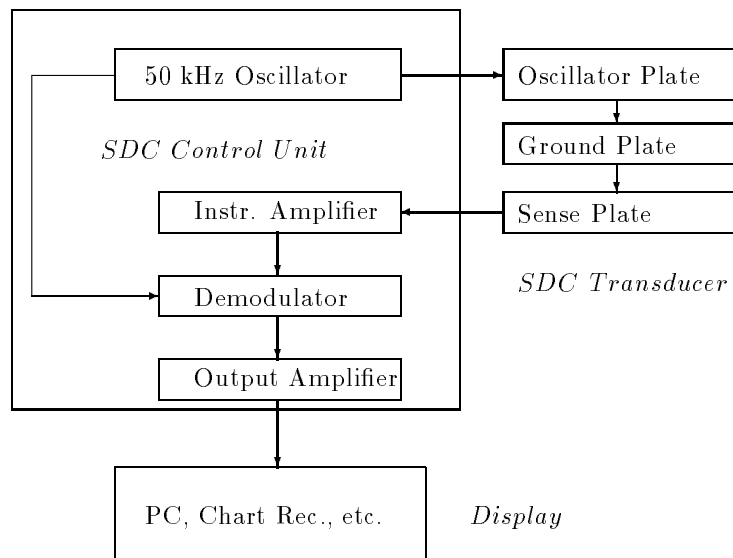


Figure 4: Block Diagram of the SDC Electronics connected to a sensor.

has been used for the study of a variety of systems, particularly low level, long period mechanical oscillations.

As noted by Braginsky, capacitors are well suited to the study of small forces in physics. Along with optical methods they offer the least perturbing influence of a system under study. Whereas optical methods can present a challenge in terms of computer automation, capacitance sensors are very compatible with the computer through A to D conversion. The force between capacitor plates can be readily calculated using energy considerations and shown, under most conditions, to be too small to be of concern. When the mechanical energies being studied are so small that the capacitor is capable of adverse influence, then the SDC devices have advantages over capacitive devices of lower symmetry. For example, as shown by Braginsky, a single capacitor will cause a different response in a system depending on whether one operates above or below resonance of the oscillator circuit of which the capacitive sensor is a part. (This is one operating mode of a capacitive sensor—enable the system being monitored to alter the frequency of a resonant circuit by changing the capacitor of the “tank” circuit. The capacitor may change by way of either area variation or gap spacing change.) Such asymmetry does not show up with SDC devices. When the sensor operates via area variation it will “harden” the system slightly (force constant proportional to the mean square voltage) because of electrostatic forces derived from the drive signal; however, there is no tendency toward instability. Additionally, the hardening can actually be a means for control by causing the position of equilibrium associated with the electrical part to be different than that of a mechanical (spring) part. The device can in this case function as an actuator. Various full-bridge capacitive devices have been used in this way, even as part of a servo (feedback) loop involving the control of very small forces [R. Peters et al, “Capacitive servo-device for microrobotic applications”, *J. Micromech. Microeng.* 1, 103-112 (1991)].

Better than the resonant circuit method, for most purposes, is one in which active capacitive elements are part of a bridge. This is the technique used in all of the capacitive sensor based products sold by TEL-Atomic, Inc. It is illustrated in the block diagram of Fig. 4.

If the bridge is used with a lock-in amplifier (implicit in the demodulator of the block diagram) then the sensitivity can be dramatically improved. This was first exploited in the work of Dicke doing microwave studies of the sun. Very few innovations of electronics have had such a profound influence on experimental physics. To assist people having limited experience with synchronous detection, the following tutorial is provided.

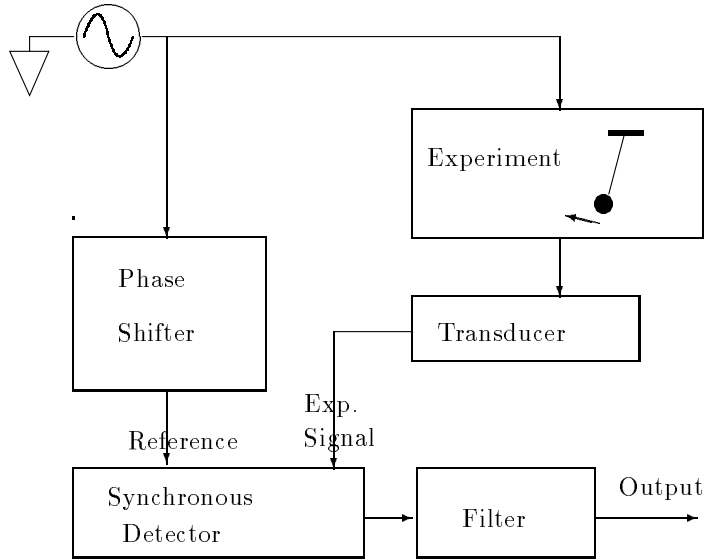


Figure 5: Block diagram of a Lock-in Amplifier.

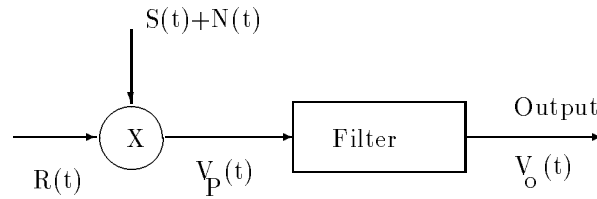


Figure 6: Operations performed by the synchronous detector.

3.6 Lock-in Amplifier

The lock-in amplifier, or synchronous detector, is the ideal electronics for bridge type sensors. As a bridge is varied through its null (balanced) position, the phase changes by 180 degrees. By utilizing this phase change, the lock-in causes the polarity of the output dc voltage to reverse sign algebraically across the null. Even if the lock-in didn't provide additional advantages of signal to noise ratio (SNR) improvement, this would still constitute a significant improvement over simply connecting a high impedance "meter" across the output of the bridge. With a meter there is a discontinuity in the slope of the output as the bridge is tuned through null. The lock-in thus increases the range of linearity by a factor of two.

The primary secret of the lock-in amplifier's success has to do with coherence, as implied by the term "synchronous" that is used to describe its operation. A reference signal in phase with the sensor drive source is utilized, as illustrated in Fig. 5.

Mathematically, the synchronous detector operates on the signal and reference signals in the manner indicated by Fig. 6.

In most actual systems, as opposed to this idealized example, the multiplication is not analog, but rather is accomplished by a switching network. The filter must then remove odd harmonics as well as performing its other essential function, described in the mathematics which follows.

For the mathematical treatment, assume that the signal and reference are harmonic, i.e.,

$$S(t) = \sqrt{2} V_S \cos(\omega_S t + \phi_S) \tag{1}$$

$$R(t) = \sqrt{2} V_R \cos(\omega_R t + \phi_R) \tag{2}$$

$$N(t) = \text{uncorrelated to } R(t) \tag{3}$$

The product is given by

$$V_P(t) = 2 V_S V_R \cos(\omega_S t + \phi_S) \cos(\omega_R t + \phi_R) + R(t) N(t) \quad (4)$$

If we use the trigonometric identity $2\cos A \cos B = \cos(A+B) + \cos(A-B)$ then we obtain

$$V_P(t) = V_S V_R \cos[(\omega_S + \omega_R)t + \phi_S + \phi_R] + V_S V_R \cos[(\omega_S - \omega_R)t + \phi_S - \phi_R] + R(t)N(t) \quad (5)$$

We follow the product with a filter whose cutoff is ω_F . Since $\omega_S + \omega_R \gg \omega_F$, and for our case $\omega_S = \omega_R$, we obtain the output result

$$V_o(t) = k V_S \cos(\phi_S - \phi_R) \quad (6)$$

so that

$$V_o(t) \propto V_S \cos \phi \quad (7)$$

where the constant, k embodies the filter attenuation. Notice that the term $R(t)N(t)$ has disappeared because the reference signal and the noise are not correlated.

For maximum sensitivity, $\cos \phi$ is adjusted to unity. In any case, the output polarity is seen to change as the output goes through zero at bridge null.

In the case of the Signetics NE5521N chip, the electronics package used with the SDC sensors; the drive signal and demodulator are all contained in one chip. Therefore, simply connecting two of the 18 pins of the DIP package injects the reference signal into the demodulator. When the sensors are used with discrete instruments (earliest work), external cable connectors are required for this task.

Most commercial lock-in amplifiers provide a phase adjusting network to insure that $\cos \phi$ be set at its maximum value. In the case of the SDC sensors, such a network has never been necessary when operating at low frequencies (about 50 kHz) with the oscillator. When using lock-ins that operate up to MHz frequencies, such a network is generally necessary.

It should be pointed out that the lock-in amplifier, although related, is not the same as a phase-lock loop (PLL). The PLL incorporates additional servo features that are not so easy to comprehend. Beautifully suited to applications in communication, it is not an instrument that normally would be a natural part of sensor technology.

The lock-in amplifier provides significant improvements in signal to noise ratio, since noise is not correlated with the reference signal. Thus it has been the instrument of choice in the past for capacitive sensors (particularly the half-bridge configuration known as "differential") and also the linear variable differential transformer (LVDT). The LVDT is a full bridge inductive sensor and has become exceedingly popular following its invention during World War II, for use in torpedoes. With the trend toward miniaturized sensors, it is expected to become less significant because it is impractical to wind really small transformers. On the other hand, its capacitive equivalent, the SDC, is very well suited to miniaturization. It is the ideal candidate for micro-electro-mechanical-systems (MEMS) integration. Interestingly, the "chip" that is used by TEL-Atomic in support of its SDC based instruments (NE5521N) is one that was designed and built by Signetics after being commissioned to do so by a prominent LVDT manufacturer (Schaevitz).

Whereas an LVDT can be connected directly to the demodulator input, capacitive sensors require, because of impedance differences, that there be an intervening instrumentation amplifier. Instrumentation amplifiers are bi-polar, as opposed to uni-polar in nature; and they have a high-input impedance. Being bipolar, an instrumentation amplifier possesses greater symmetry than a unipolar amplifier. This symmetry is the reason for their common-mode-rejection advantage, which is possible because the pair of input lines carry experiment signals that are of opposite polarity (differential) with respect to ground. A noise signal that should be coupled to the input (because of inadequate shielding) will usually have nearly the same magnitude, and phase, in each of the two lines; i.e., the signal is "common" to the pair. The instrumentation amplifier is designed to respond to the differential signal (experiment) and suppress the common signal (noise). The quantifying of its selectivity in dealing differently with these two signals is referred to as the common-mode-rejection ratio (CMRR). Typically, the CMRR for an amplifier such as used in the TEL-Atomic apparatus is better than 40 dB. The decibel, for voltage work,

is defined as 20 times the logarithm (base 10) of the voltage ratio. Thus the noise signals of common type are attenuated by a factor of more than 100 as compared to the experiment signal.

In the earliest work with full-bridge capacitive sensors, separate components were employed. For example, one oscillator that worked very well was the vacuum tube instrument which was probably the first product of the Hewlett-Packard company. The stability of these early instruments, following warm-up, proved better than any of the solid state electronic oscillators that were also tried. This is because their phase noise is less, an important consideration for lock-in amplifiers. The lock-in amplifiers which were most effective in this early work were the old Princeton Applied Research (PAR) analog instruments, which outperformed newer and more expensive digital ones. Perhaps it is worth asserting at this point, that “newer” is not always “better” in physics instrumentation, and digital systems are not always better than analog ones. Nor are solid state devices always preferable to vacuum tube technology. A case in point has to do even with voltmeters connected to the output of the SDC electronics to visually monitor a slowly changing system. Digital voltmeters are not nearly so useful as an old analog voltmeter for this purpose.

There’s a definite advantage to putting all electronics onto a single, compact PC-board. As demonstrated with the TEL-Atomic package, there are improvements in stability which results, both thermal and mechanical, because of the small size. This is reminiscent of the improvements in performance of scanning tunneling microscopes as they were miniaturized. One of the greatest challenges to the development of the first STM by Binnig and Rohrer was to isolate the unit from vibrations. By reducing the size, and thus moving the characteristic frequencies to higher values, there has come a considerable improvement in the performance of STM’s.

The biggest problem facing capacitive sensors in the past was the difficulty of dealing with problems that derive from typically large output reactance. Attempts to combat this by increasing the frequency of the drive met with little success. Attempting to compensate by increasing the size of the drive voltage is not a viable solution either, particularly when dealing with modern electronics. The invention of the field effect transistor was of major importance for capacitive sensors, particularly as FET’s were incorporated into integrated circuits, such as the QUAD-JFET (LF347N) used in the the TEL-Atomic electronics. The high input resistance and acceptably low input capacitance of this chip are definite assets to any capacitive sensor. The instrumentation amplifier which uses them is one which provides an additional dramatic improvement for capacitive sensors—a large CMRR ratio.

The SDC sensors have been constructed in a variety of configurations. Some measure rotation, others translation, and still others deformation. Many of the ones that have been built are topologically related. For example, one can readily envision how to convert some sensors with planar geometry to related configurations with cylindrical geometry. Prof. Valery Serbo of Novosibirsk State University in Siberia referred to the configuration described in this document as a “crucial” invention for the research conducted in the new field of mesoanelastic complexity. The word “crucial” is appropriate on two accounts—first, it is the most generally useful of the configurations presently known; and second, the insulator gaps in one set of the pair of static electrodes actually form a “cross”. The recent allowance of claims on the patent application for the SDC sensors is also the result of this cross connection of electrodes (as mentioned by patent examiner, Chris Tobin). (Being a Christian, whose creativity has been inspired of the Holy Spirit, this has been significant to me.)

The sensor uses two static electrode sets and a rectangular shaped conductor (relatively thin) which moves between them as shown in Fig. 7. In the usual arrangement, the ac drive (about 50 kHz) is applied to the quad set of plates. These are cross-connected to form two equipotentials. The rectangular static pair are connected to the instrumentation amplifier, which is followed by the synchronous demodulator. The device operates by area variation between the static electrodes on opposite sides of the moving electrode. Because charge cannot be induced through the high conductivity (aluminum normally adequate) moving electrode, the areas that would otherwise be capacitively coupled, are shielded from one another by whatever portion of moving plate that should be between them. If one ignores edge effects (shown through the years to be a reasonable approximation in most cases), then the equivalent circuit of the sensor is as shown in Fig. 8, and can be obtained by inspection.

Nominally, components on opposite sides of the bridge maintain the same capacitance as they change, and adjacent components of the bridge differ in algebraic sign. The symmetry is such that the output

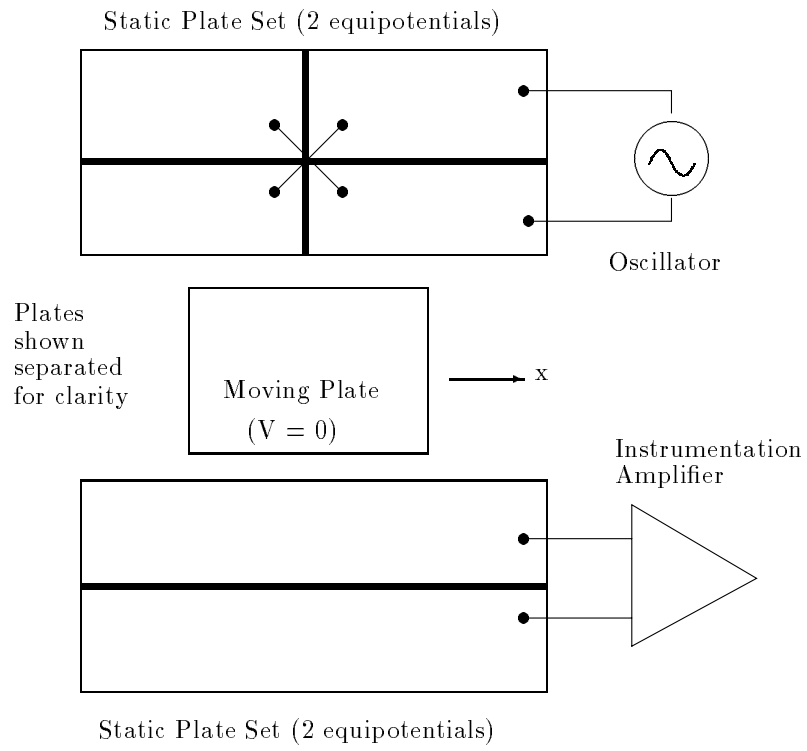


Figure 7: SDC Planar Geometry Position Sensor.

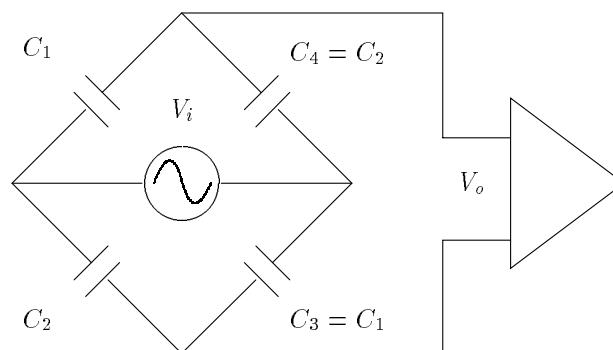


Figure 8: Equivalent circuit of the SDC Sensor.

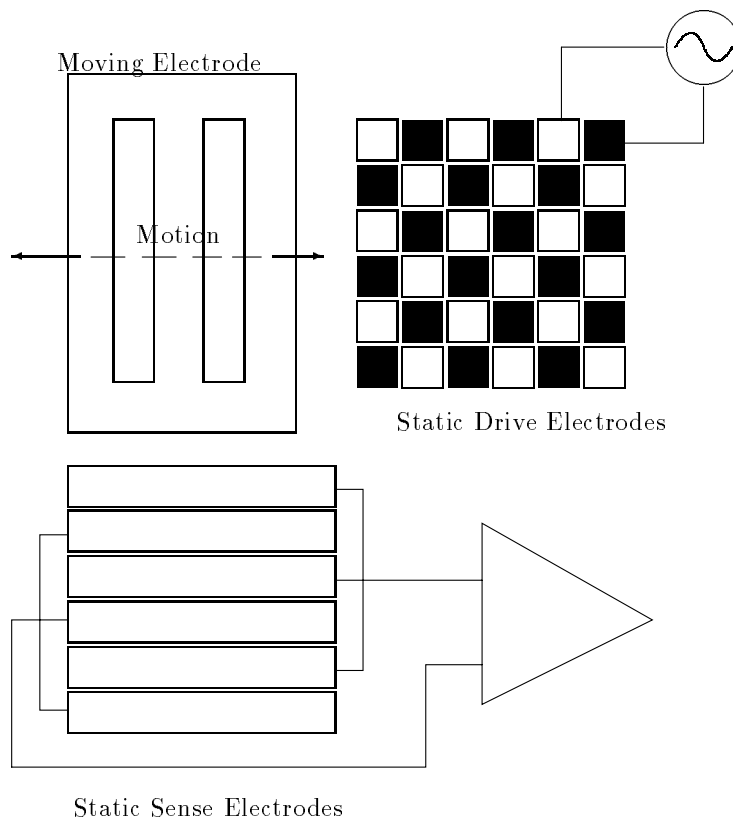


Figure 9: An array for measuring linear position. (The electrodes are shown separated for clarity.)

from the device (dc voltage out of the amplifier following the synchronous detector) can be expressed as $\frac{V_o}{V_i} = 2 x / L = \frac{C_1 - C_2}{C_1 + C_2}$ where L is the length of the moving electrode.

The fact that the output is proportional to the ratio of the difference to the sum of the unique capacitances of the bridge is significant. It means that the sensor possesses an invariant to scaling property. Of course the reactance of the Thevenin output equivalent circuit increases as the size of the sensor decreases. This can be offset by placing the instrumentation amplifier closer to the sensor to reduce stray capacitance (the input resistance of any FET is large enough that the reactance would have to get really big before becoming a problem).

For measuring small motions, the SDC detector can be constructed in the form of an array of sensors. Two examples are provided in Figures 9 and 10. The array of Fig. 9 is one that is used for linear position sensing, whereas that of Fig. 10 is for angle measurements. Prototypes of both have been tested. The angle array could be especially useful in a sensitive tilt meter.

The sensitivity of a single sensor is inversely proportional to the length of the moving member (dimension in the direction of motion). If the range of measurements is extremely small, then this dimension can be made accordingly small, with a dramatic increase in sensitivity. If a single sensor were used, there would be a resulting unacceptably large output reactance. Although the sensitivity, in the absence of output reactance, would go to infinity as this dimension goes to zero; in fact the loss due to reactance becomes eventually greater than the gain due to reduction of the dimension. By connecting several sensors in parallel, each of which responds the same way to the observable, this loss is overcome. As the dimension becomes progressively smaller, the number of individual sensors required becomes larger. The output reactance does not increase because the overall area (parallel connection) remains virtually constant. Operationally, one operates the array where the slope of the output vs motion is greatest. When there's a large number of sensors this slope is correspondingly large, reminiscent of the manner in which optical resolution (through interference) is improved by going to multiple slits instead

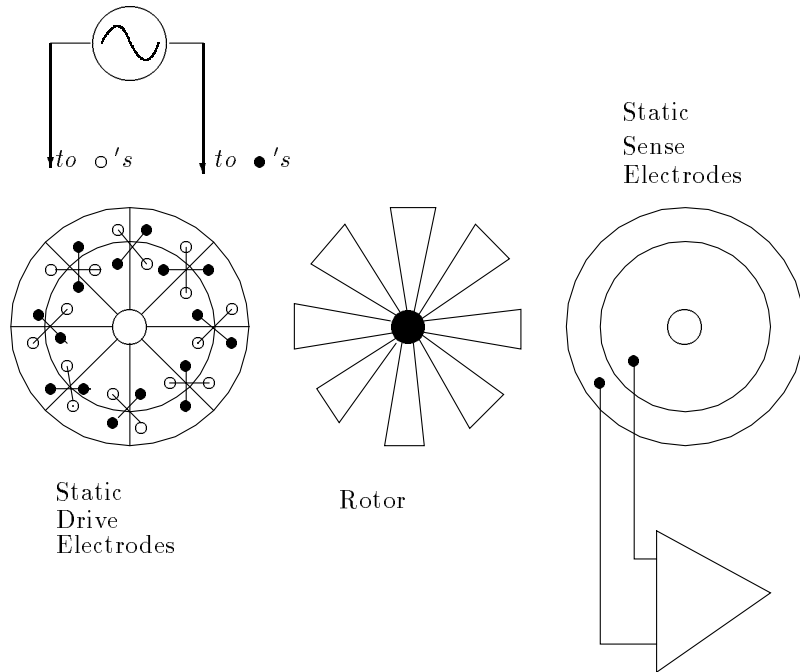


Figure 10: An array for measuring angular position. (Electrodes shown separated for clarity.)

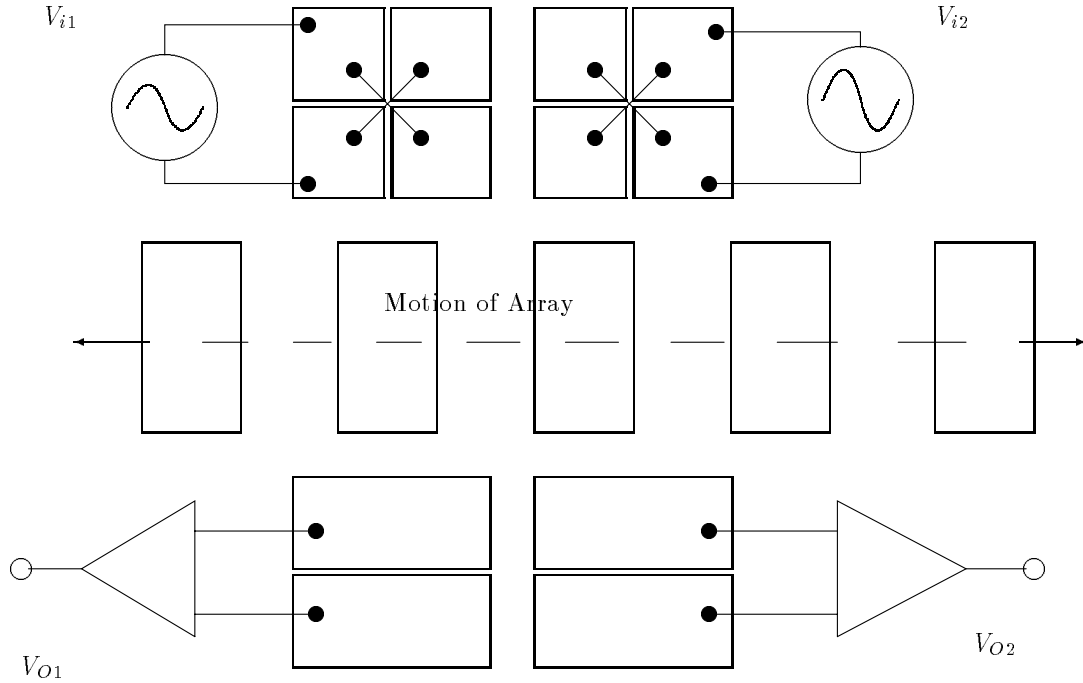
of using a single slit or a Young’s experiment pair. As a grating is far superior in the optics case, in similar manner a very large number of small dimensioned capacitive sensors could produce enormous sensitivity compared to a single unit.

It’s also possible to configure sensors in an array so that there are no range limitations. For example, Fig. 11 shows a linear position sensor with unlimited range. An infinite range angle measuring transducer which is similar has been described in the literature [R. Peters, “Capacitive angle sensor with infinite range”, *Rev. Sci. Instrum.* 64 (3), 810 (1993)].

With regard to stray capacitance, the SDC sensors have a dramatic advantage. The full-bridge symmetry means that stray capacitance tends to have an equal influence on each of the bi-polar lines from the sensor to the instrumentation amplifier. This common mode noise is significantly attenuated as compared to the desired differential (experiment) signal from the sensor. When using a lower symmetry device, such as the standard differential capacitive sensor, there is less common-mode rejection. Because the fixed capacitors (or inductors when using a ratio transformer) which are added to complete the bridge are not part of the sensor proper, there is a higher probability of noise getting through. Older capacitive sensors required that a great deal of shielding be generally used lest changes in stray capacitance severely upset the unit (such as by putting one’s hand close to the apparatus). The SDC sensors are dramatically less susceptible to these effects. In some cases very little shielding is required, which is virtually unheard of in the past.

It can be shown (see Appendix IV) that an SDC sensor (alternatively called doubly differential) has twice the sensitivity of a conventional differential capacitive sensor of the same size; i.e., equal electrode areas, total. This factor of two applies when the input capacitance of the instrumentation amplifier, including cables (call it stray) is negligible compared with the output capacitance (Thevenin equivalent) of the sensor. As the stray capacitance increases, the factor of 2 reduces toward 1; and the output becomes proportional, when the stray is large, to the ratio of sensor capacitance to stray capacitance. The SDC sensor is always the more sensitive of the two, no matter how much stray capacitance is present.

There’s an interesting story behind the “crucial” SDC configuration. A system had been constructed to look at changes in the period of a leaky pendulum. The first studies of this leaky pendulum were ones which used an LRDC sensor positioned at the support axis near the top of the pendulum. Because



Plates shown separated for clarity

Figure 11: Illustration of an array for unlimited range measurement.

the amplitudes of oscillation studied were small, it was deemed preferable to consider a different type of sensor placed at the bottom of the pendulum. It was decided to glue a glass microscope slide to the bottom end of the pendulum and let this move between static plates (constructed of PC-board). This worked reasonably well and was recognized to depend functionally on the difference in the dielectric constants of air and glass. Thus it was reasoned that replacing the slide with a rectangular piece of silicon (pre-integrated-circuit wafer) should give about a three-fold improvement in performance, due to the larger dielectric constant. What was found was a much larger improvement than expected, because the silicon was highly conductive, due to doping. Thus the “crucial” SDC using a metal “slide” was discovered by serendipity. Subsequently it was discovered that this particular sensor could be topologically altered to build a better angle measuring sensor than the original LRDC sensor. It still has no mechanical contact (such as by brushes or twisting wires) with the rotor, and both the range and sensitivity are significantly larger than that of the earlier sensor.

3.7 Electronics

The timer used to control the drive frequency of the TEL-Atomic MPCP is a very common and inexpensive one, the LM555. This is a device which is typically used to provide pulses. If connected as shown in Fig. 12 the output is a square wave; i.e., the on and off times of the voltage at pin 3 are equal. This requires that the switchable resistors, R_A and R_B , (selected by SW4A and SW4B) maintain a constant ratio in their values (A being the larger of the two) that is always nominally 42%. The frequency of the timer is determined by an RC product, C in this case being $4.7 \mu F$. By going to a relatively large value of C, the desired frequencies in the neighborhood of 1 Hz are generated without having to use inordinately large resistors.

Obtaining position information for the pendulum is a simple matter of electronically integrating the output from the velocity sensor. This is done with a MOSFET LF356 operational amplifier as shown

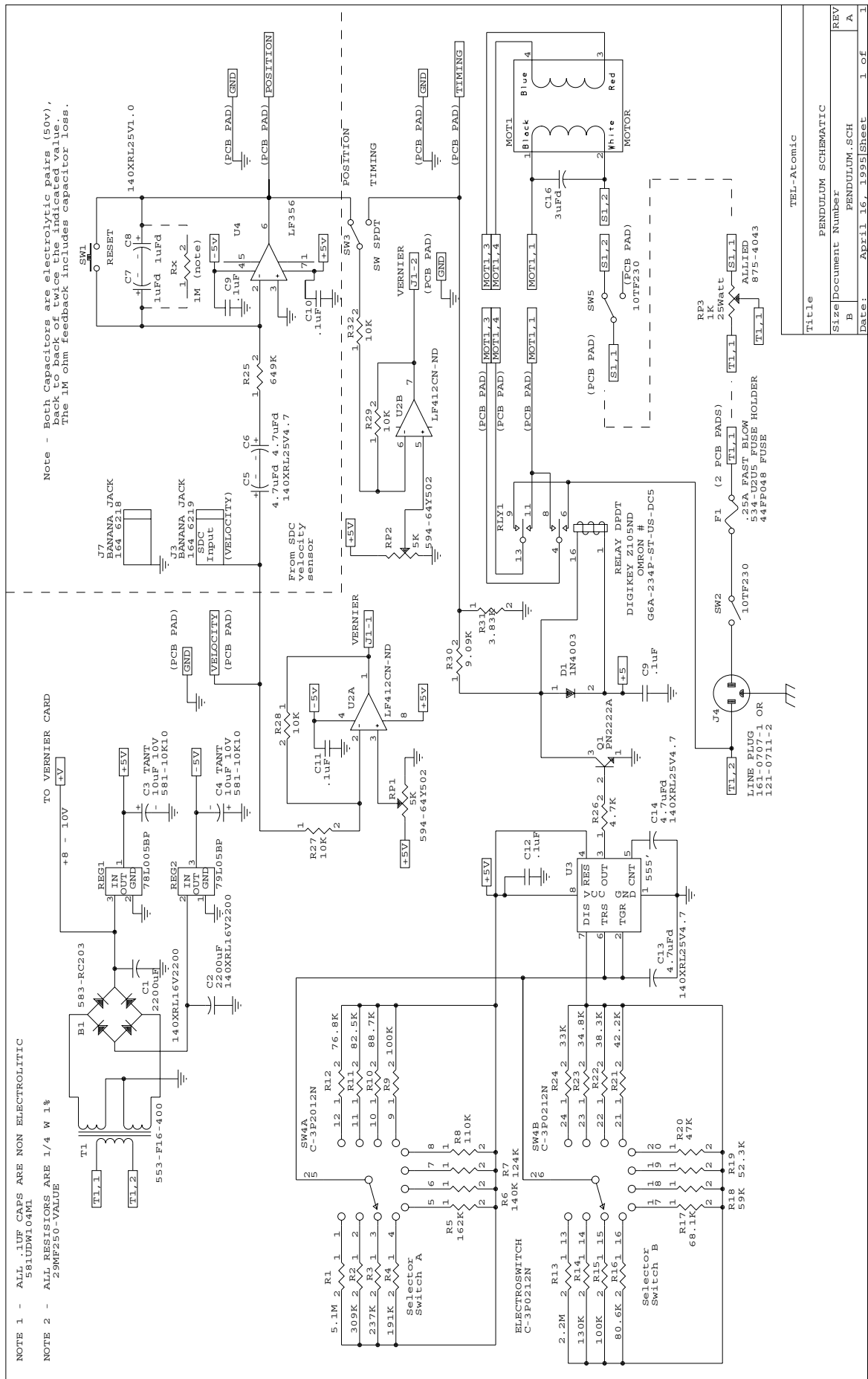


Figure 12: Electronics used in the Multi-Purpose Chaotic Pendulum.

in Fig. 12.

For ease of operation the integrator uses a bi-polar power supply (equal + and - with respect to ground). Attempts to make the system function properly with a cheaper unipolar supply were not successful. The integrator is, by design, what is referred to as “leaky”. Even if the feedback capacitor ($0.5 \mu F$) were not shunted by the indicated resistor, there would still be leakage; i.e., the capacitor is not perfect, rather it has 10’s of Megohms shunt resistance. The “leak” keeps the voltage corresponding to position from saturating when the pendulum is in a “winding” mode.

The 555 timer is not capable of supplying, by itself, the power required to close the contacts of the motor relay. Thus an inexpensive, low-power NPN transistor (PN2222) has been placed between the timer and the relay coil as shown in Fig. 12. Opening of the relay contacts would result in significant (undesirable) voltages across the transistor (from the rapidly decaying flux of the coil) except that the coil has been shunted with the diode shown. A resistor is shown in the base circuit of the transistor. This was selected according to the size of the voltage delivered from the timer, which depends in turn on the size of the power supply voltage.

Additionally pictured in Fig. 12 are components that control the output torque (including direction) of the motor. The reversal of direction of the torque is accomplished with the DPDT relay. Assume that switch position “A” corresponds to the normally open position of the relay; then zero coil current results in the $3 \mu F$ capacitor being placed in series with motor winding 1. The resulting motor torque is in one direction at constant magnitude—call it clockwise. If the coil is energized as the result of a positive voltage from the timer being applied to the base of the PN2222, then the relay closes and the $3 \mu F$ capacitor is now placed in series with motor winding 2. Thus the output torque is changed to counterclockwise with a magnitude that is essentially independent of rotor position.

Observe that the magnitude of the motor torque is controlled by the amount of current delivered to it. This is regulated by the amount of resistance placed in series with each of the windings (through the 25 W rheostat, RP3). Whether from a rheostat or by switching in fixed components, the resistors must have a large enough power rating to dissipate the Joule heat. Although, as mentioned earlier, a more elegant control scheme would be one which utilizes a saturable core reactor to avoid Joule losses, the present scheme is acceptable, since the motor power requirement is low.

4 The Computerized Pendulum

4.1 General

Before conducting the exercises mentioned in this section, it is recommended that a review of the theory of the simple harmonic oscillator (SHO) be performed. In particular, one should be familiar with the concept of the log-decrement of dissipated motion. The SHO is an example of a linear system. When the equation of motion contains nonlinear terms, things can be dramatically different. In the first place, superposition no longer applies; which causes severe mathematical limitations. The best way to deal with most nonlinear problems is through computer modeling, since many common analytic techniques (like the Laplace transform) can not be used.

A system that is nonlinear may exhibit chaotic motion. Nonlinearity is a necessary but not sufficient condition for chaos. For example, the TEL-Atomic MPCP can exhibit a highly nonlinear motion (the “bell-ringer” mode) that is periodic (refer to Fig. 23, pg.33). If it is driven in such a manner that motion past vertical is allowed, then chaos can occur for some combinations of drive amplitude and frequency relative to the pendulum’s natural (low level) frequency and damping.

The best tools for studying chaos, where sensitive dependence on initial conditions is present, are ones which were developed years ago. Since students are especially familiar with time records, one display mode we’ll use is that in which both pendulum displacement and velocity are plotted vs time. This is a good one for measuring the log-decrement of the motion.

4.2 Algorithms

REPRESENTATIONS

It is recommended that one initially learn (or review) some fundamental concepts with the TEL-Atomic software (‘TELAWARE’) before connecting the pendulum to the computer. The software for these activities is a subset of the HARDWARE INTERFACE MENU (HIM). To access the appropriate algorithms, press ‘H’ from the ‘TELAWARE’ menu, and then ‘P’[return] from the menu which follows. Within the resulting PENDULUM SIMULATIONS MENU (PSM) are the following 6 options:

- (1) Phase space trajectory, standard
- (2) Phase space trajectory, MPCP
- (3) Displacement & velocity vs time
- (4) Poincare’ section, standard
- (5) Poincare’section, embedding theorem based
- (6) Bellringer (or other) mode (providing for FFT).

Since people are generally most familiar with temporal records, PSM program (3) is probably a good starting point. The prompts before execution permit entry of system parameters. One may simply press [enter] after each prompt to use the default values. Fig. 13 shows a typical response—based on the default set.

Notice that the displacement and velocity are 90 degrees out of phase with each other, after steady state has been reached—assuming sinusoidal motions (small amplitude). The velocity (blue curve on the monitor—here smaller at steady state) is provided primarily for reference purposes; there is no ordinate scale of numbers in rad/s. Program (3) is not well suited to investigations of chaotic motion. The parameters could be adjusted to attain chaos, but keeping the graph on the screen would require software features that are not worth the effort. We’ll see that the phase space plots are much better, in general. One of the useful things that can be done with program (3) is to hold everything constant except drive frequency, and then tune through resonance. After waiting for the transients to settle, the amplitudes can be read individually from the screen and then plotted. The resulting Lorentzian is well known (for small drive amplitudes), since this approximates the resonance response of a simple harmonic oscillator. One can generate curves of this sort with different damping constants to show how the half-width of the response changes with the “Q”.

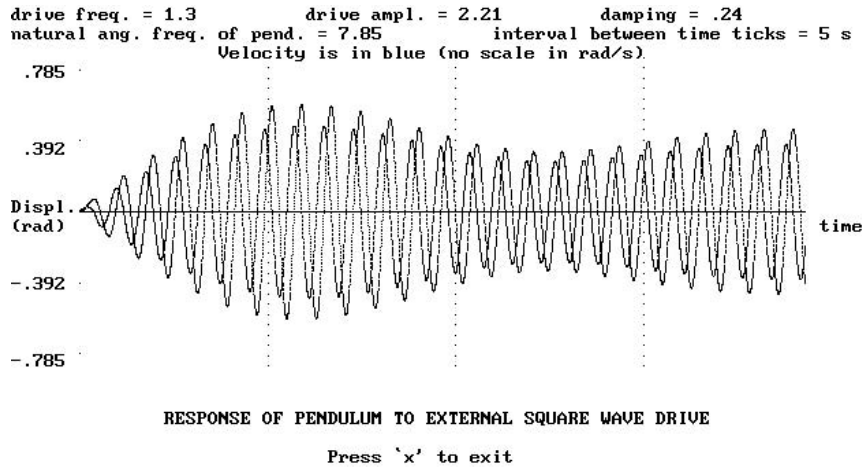


Figure 13: Example output from program (3) of the Pendulum Simulations Menu.

One who is interested in comparing a given pendulum with the simulation should, in most cases, refer to TABLE I, which is the source code of program (3). The numbers, which correspond to the first MPCP prototype, serve as a useful example.

TABLE I: PENDULUM SIMULATION

```

REM Quickbasic LPA program simulating approach (with transients) of the
REM pendulum to steady state (non-chaotic) for constant drive.
REM The constants correspond to an early MPCP prototype. REM ad = amplitude of the drive torque
REM f = drive frequency
REM c = damping constant (different for different pendulum lengths)
REM w0 = pendulum's natural angular frequency
REM Shift F5 to execute
REM Ctrl Break to exit
SCREEN 9
COLOR 15, 4
CLS
fx = 1.3: w0x = 7.85
pi = 3.1416: adx = 2.21: cx = .24: tpi = 2 * pi
PRINT "you may simply press [enter] to obtain default for any case"
PRINT "input drive frequency (Hz) (.5 to 1.5)"
INPUT f
PRINT "input drive amplitude (0.1 to 5)"
INPUT ad
PRINT "input damping coefficient (.05 to 5)"
INPUT c
PRINT "input natural ang. freq. of pendulum (1 to 10)"
INPUT w0
CLS
IF f = 0 THEN f = fx
IF ad = 0 THEN ad = adx
IF c = 0 THEN c = cx
IF w0 = 0 THEN w0 = w0x
w = tpi * f
VIEW (50, 0)-(600, 300): WINDOW (-0, -.4)-(.4, .4)
dt = 2 * pi / 2000

```

```

tr = 20
j = 0
100 CLS: IF t > tr THEN j = j + 1
LOCATE 24, 30: PRINT "Press 'x' to exit";
LOCATE 11, 1: PRINT "Displ.";
LOCATE 12, 1: PRINT "(rad)";
LOCATE 12, 75: PRINT "time";
PSET (0, .35 * pi / 8): PSET (0, -.35 * pi / 8)
PSET (0, .35 * pi / 4): PSET (0, -.35 * pi / 4)
LOCATE 8, 1: PRINT .001 * INT(1000 * pi / 8)
LOCATE 4, 1: PRINT .001 * INT(1000 * pi / 4)
LOCATE 1, 1: PRINT "drive freq. ="; f
LOCATE 1, 28: PRINT "drive ampl. ="; ad
LOCATE 1, 55: PRINT "damping ="; c
LOCATE 2, 1: PRINT "natural ang. freq. of pend. ="; w0
LOCATE 2, 45: PRINT "interval between time ticks = 5 s";
LOCATE 3, 20: PRINT "Velocity is in blue (no scale in rad/s)";
LOCATE 22, 15: PRINT "RESPONSE OF PENDULUM TO EXTERNAL SQUARE WAVE DRIVE";
LOCATE 15, 1: PRINT -.001 * INT(1000 * pi / 8)
LOCATE 19, 1: PRINT -.001 * INT(1000 * pi / 4)
REM loop for updating the time and integrating the canonical equations
start:
t = t + dt: q = SIN(w * t)
REM next pair of eqns. converts from sine to square wave drive
IF q > 0 THEN q = 1
IF q < 0 THEN q = -1
REM the next pair of eqns. updates the angular momentum
dpdt = -w0 * w0 * SIN(th) - c * pq + ad * q
pq = pq + dpdt * dt
REM the next eq. updates the angle
th = th + pq * dt
PSET (.02 * tp, .35 * th)
PSET (.02 * tp, .035 * pq), 3
PSET (.02 * tp, 0)
IF tp < .2 THEN GOTO 200
IF ABS(.2 * tp - INT(.2 * tp)) > .001 THEN GOTO 200
FOR l = 1 TO 15
PSET (.02 * tp, .02 * l)
PSET (.02 * tp, -.02 * l)
NEXT l
200
tp = t - j * tr
IF tp > tr THEN GOTO 100
GOTO start
END

```

HARDWARE ROUTINES

There are 5 hardware interface routines for the MPCP. They are selected individually from the HARDWARE INTERFACE MENU (HIM). They are as follows:

- (1) Phase space trajectory
- (2) Velocity and displacement vs time
- (3) Poincare' section

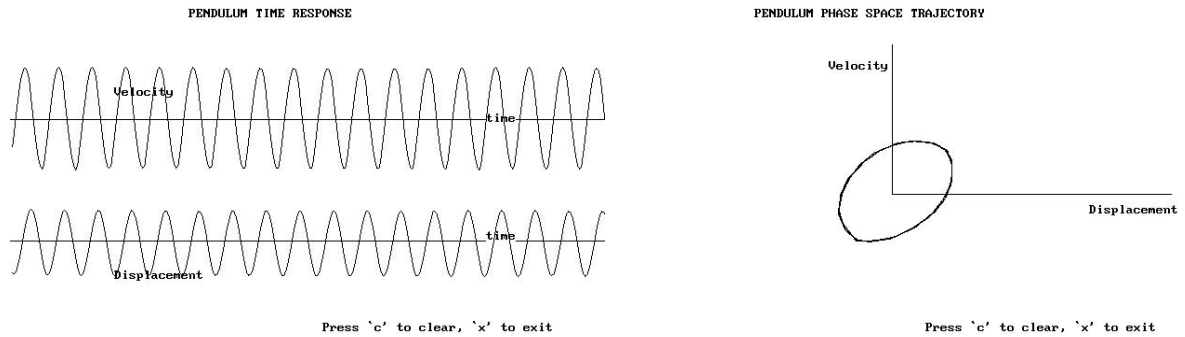


Figure 14: Example output from the pendulum—both graphs for a period-1 limit cycle.

(a). Time history of the motion

(b). Phase space trajectory

- (4) Drive cycle timing relative to velocity
- (5) Same as “2” except that the velocity is stored in memory so that the power spectrum can be generated.

The Fig. 13 graph (simulation generated) can be readily compared to the actual pendulum. In the HIM MENU, enter (2). Shown in Fig. 14a are velocity and displacement time records of the MPCP in a periodic motion at fairly low level.

4.3 Phase Space

One of the most useful graphical representations in all of physics is that in which momentum (or velocity) is plotted against displacement. In Hamilton’s terminology, we would say that the momentum, p , conjugate to q is plotted vs q ; where q is a generalized coordinate. It might be a linear variable (such as x), or an angle (such as θ), or almost anything. In the case of a SHO, this p vs q plot is an ellipse, if the motion corresponds to steady state. In the case of the pendulum, as the amplitude gets large, the ellipse becomes distorted. When the oscillator is not driven, and there is damping; then the phase space trajectory is a logarithmic spiral (c.f. Marion). This can be demonstrated easily with the MPCP by establishing a steady state, and then turning off the drive with the appropriate switch.

When the drive is large enough for chaos, the bob will sometimes go past vertical. This causes a problem with the display, because a secular term can drive the graph off-scale (and/or saturate the electronics in the hardware). Traditionally, this problem is addressed by mapping the angle into $\pm\pi$ by means of the modulo operator. (Textbooks have far too little to say about this important mapping operation, so the following software program is included—It maps any input value of θ into $\pm\pi$.

```

REM Maps theta into the range -pi to pi
REM Shift F5 to start, ctrl Break to exit
start:
CLS
PRINT "input an angle greater than pi to see how it is mapped into +/- pi"
INPUT theta
tpi = 6.2832
qr = ABS(theta) / tpi: qri = INT(qr)
qd = (qr - qri) * tpi: IF qd > tpi / 2 THEN qd = qd - tpi
IF q < 0 THEN qd = -qd
thetan = qd
PRINT thetan
SLEEP 4

```

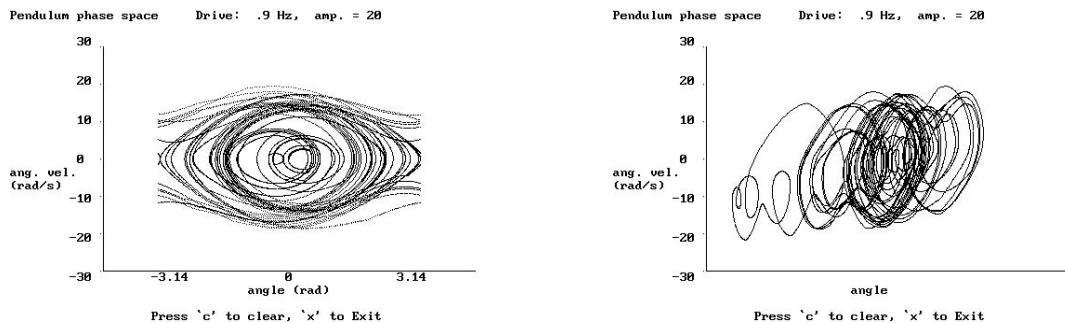


Figure 15: Example software generated Phase Space trajectories of the pendulum.

(a). Conventional

(b). Simulation of the MPCP

GOTO start:

In the case of the MPCP, it was not convenient to do this. Instead, a “leaky” integrator became the solution of choice; where the integrator is in the hardware, in the form of an operational amplifier with a feedback capacitor. The displacement of the pendulum is, of course, simply related to its velocity—one need only integrate velocity to obtain displacement. This is especially relevant, because (as noted in the description of the apparatus) the MPCP motion is measured with a velocity sensor. To keep the phase space plot confined, the charge on the feedback capacitor is continuously drained through a resistor (time constant of a few seconds)—thus the origin of the term, “leaky” integrator. In some other chaotic pendula, such as the one sold by Daedalon; the motion sensor is based on position (angle). Thus the modulo 2π operation is, of necessity, an integral part of the measurement process. Such techniques are naturally suited to digital methods, as opposed to the analog ones employed in the MPCP. Nothing in the way of digitization is done in the MPCP before serializing the data. The serial interface (made by Vernier of Portland, Oregon) operates real-time on the voltages which are proportional to angle and angular velocity.

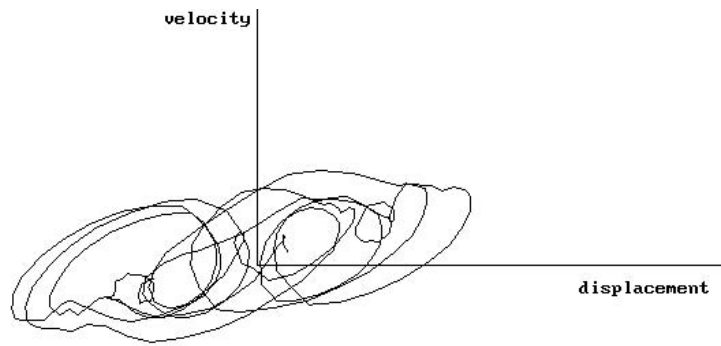
It should be noted that there is an artifact of the “leaky” integrator. Because of the associated time constant, the voltages corresponding to displacement and velocity are not quite 90 degrees different in phase. For example, consider a period-1 limit cycle produced with HIM program (1), as shown in Fig. 14b. Ideally, the major axis of this ellipse should be aligned with the displacement axis, which it is not. The non-zero inclination derives from the integrator delay time.

To compare phase trajectories (standard vs present system), one may run PSM programs (1) and (2). Sample results for identical pendulum conditions are shown in Fig. 15.

In Fig. 16 is a phase space plot (chaotic) generated by the pendulum. This plot was obtained using HIM program (1).

As previously noted, simulation of the pendulum’s chaotic time records would require a modification to program (3), which was not done. Simulating the “leaky integrator” approximation to the displacement would be straightforward enough, but this was not done. Nevertheless, one can readily study chaotic temporal records with the pendulum. For example, Fig. 17 shows a chaotic record corresponding approximately to the motion that produced Fig. 16. For “scaling” of graphs such as these, one may conveniently change gain settings on the SDC electronics.

In general, it is difficult to extract useful information from temporal records. In the case of nonlinear systems, even periodic motions can be complicated enough that the time records are difficult to evaluate. In such cases, the phase trajectory or Poincare’ section is more useful. A case in point is the period-5 limit cycle shown in Fig. 18. Period-5 means that the pendulum takes 5 times as long to repeat its motion as does the drive. It’s hard to see the $1/5$ th subharmonic in Fig. 18a, although it becomes obvious when studied by Poincare’ sectioning. It is obvious because of the 5 separate groups, which would be points in the absence of noise.



Phase Space trajectory

Figure 16: Example output from the pendulum—a chaotic phase space plot.

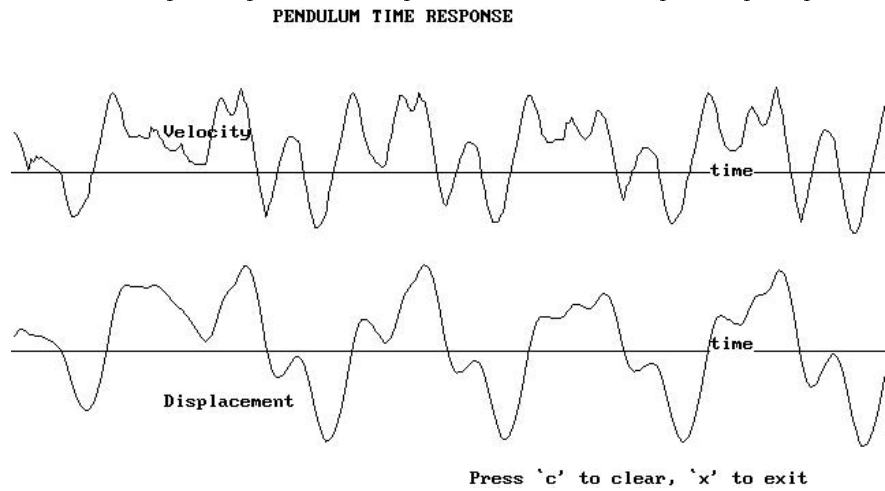
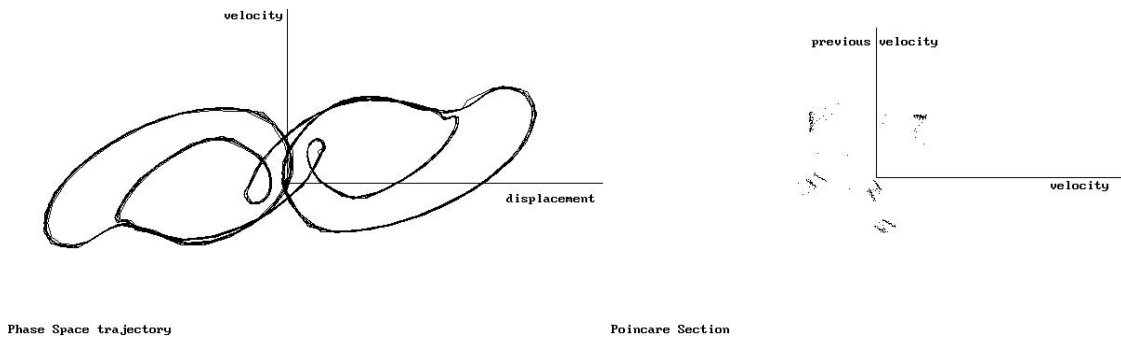


Figure 17: Example chaotic time records generated by the pendulum.



Phase Space trajectory

Poincare Section

Figure 18: Pendulum generated graphs—period-5 limit cycle.

(a). Phase space trajectory

(b). Poincaré section

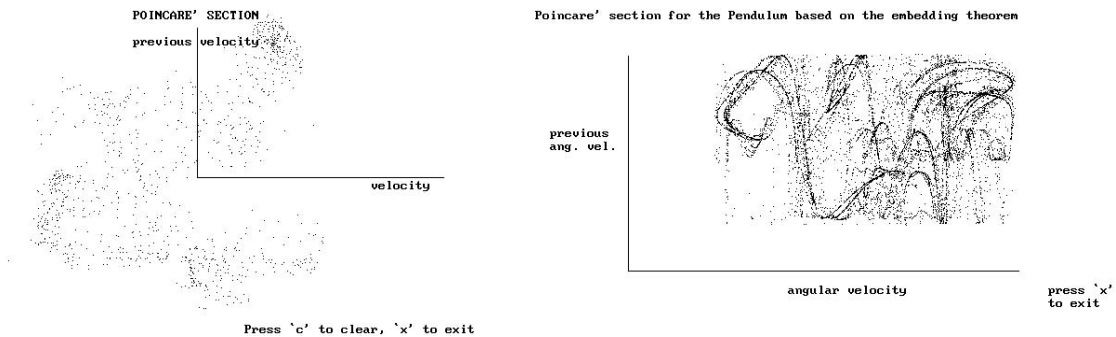


Figure 19: Poincaré sections corresponding to chaos.

(a). MPCP generated

(b). Simulated—embedding based

4.4 Poincaré' Sections

The phase space for periodic motions is “uncluttered”; however, when the motion is chaotic, this space becomes too “busy” to be useful. Additionally, for long period subharmonics, the “folding” within the phase space (loops within loops) makes it hard to know what the order of the subharmonic is. The Poincaré section removes these difficulties. To generate the Poincaré section, one “strokes” the phase trajectory, once per drive cycle. This has been done in generating Fig. 18b, which corresponds to the same motion as recorded in Fig. 18a. It was obtained by using HIM program (3).

The Poincaré section is also the best way of studying chaotic motion. Points of the section fall on what’s called a strange attractor having fractional dimension (or fractal, following Mandelbrot). Fig. 19a shows the early accumulation toward a fractal. It was obtained with program (3). When the number of points in the graph gets large enough (several thousand), the self similarity of the attractor becomes visible.

It is useful to compare the fractal generated by the pendulum to that produced with the software PSM program (5). The simulation case is shown in Fig. 19b. Because the collection time was short, there are not enough points in Fig. 19a to make a useful comparison. Additionally, it should be noted that a near perfect correlation between theory and experiment would be extremely difficult—due to the very nature of chaos.

Notice that the Poincaré sections have been obtained using the embedding theorem, also referred to as a delay construction; since the angular velocity one drive cycle earlier is plotted versus the present angular velocity. It is similar in this respect to the return map of the logistic equation program #27 of the GENERAL SIMULATIONS MENU (GSM). The pendulum has a larger number of variables, however; so the result is much more complex.

The more common Poincaré section for the pendulum is obtained by plotting velocity vs displacement. It requires that the angle be mapped into $\pm\pi$. As mentioned earlier, this is not easily done with the MPCP. With the computer, however, one can readily generate the well known section shown in Fig. 20 [made with PSM #4]. It should be noted that this commonly known figure is only one of an infinity of possibilities according to the phasing of the “strobe pulse”.

POWER SPECTRA

It also should be noted that the HARDWARE INTERFACE MENU provides for power spectral analysis of actual pendulum motion. HIM program (5) stores 1024 points (1K) into memory, so that the fast Fourier transform (FFT) may be used to obtain the power spectrum. The FFT algorithm is GSM Program #26, so that a change of menu is necessary for use. After the interface program “times out” (total time of 20 s), change to GSM and execute program #26. Example pendula spectra (one periodic and the other chaotic) are shown in Fig. 21. It was the velocity, rather than displacement, that was stored for spectral analysis.

In a more general pedagogical sense, the pendulum apparatus is also very useful; i.e., one may improve one’s understanding of spectrum analysis without even considering pendulum motion. The output from

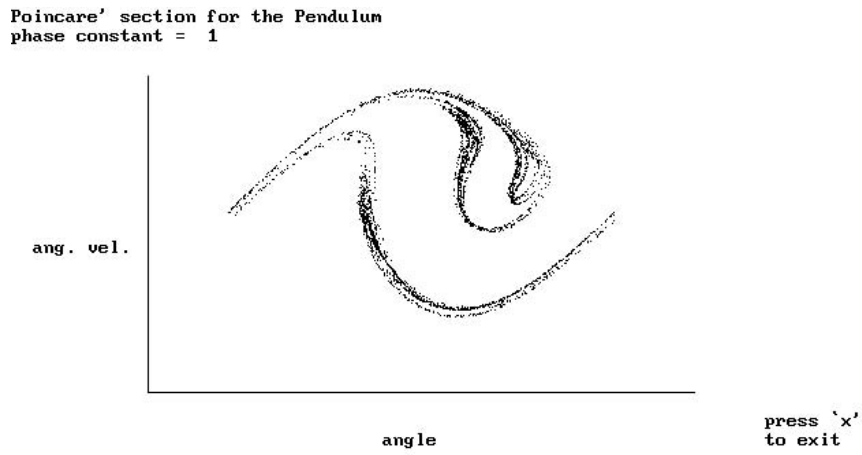


Figure 20: Simulated Poincaré section (standard) corresponding to chaos.

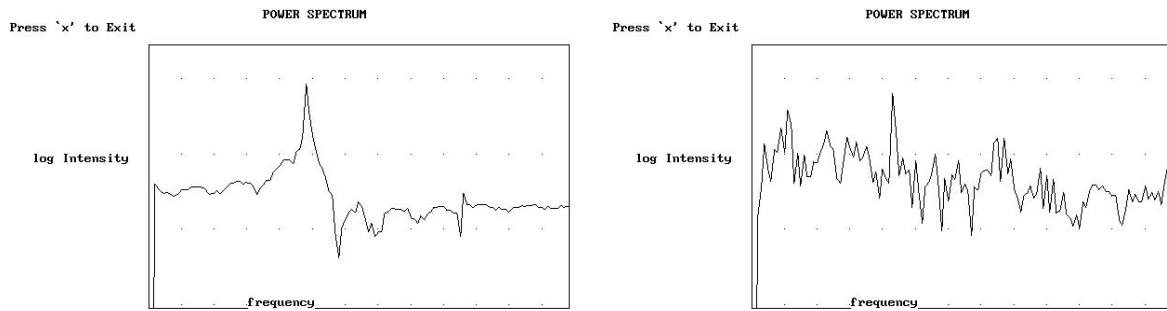


Figure 21: Power spectra using HIM program (5), followed by GSM program #26.

(a). Periodic motion case

(b). Chaotic motion case

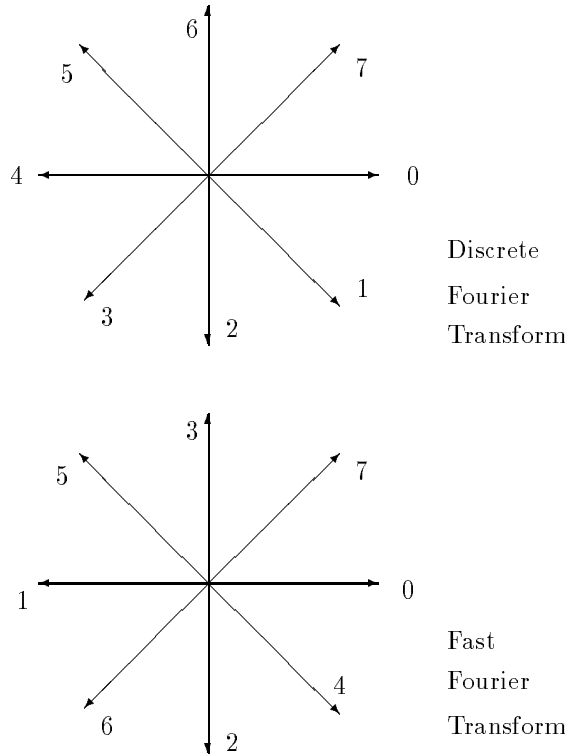


Figure 22: Order of calculations in the Fourier Transform.

a signal generator (level of about 0.5 V) is fed into the MPCP box, where the SDC control unit output normally goes. By using different wave forms sequentially—such as sinusoidal, square wave, triangular, and sawtooth; the harmonic content of the different types can be readily studied. Most people do not have an intuitive sense of the frequency domain, so this exercise can be very helpful.

Execution time in general, for the Cooley-Tukey FFT algorithm, is worth noting. It is proportional to $N \log N (\text{base } 2)$ as opposed to N^2 for the discrete Fourier transform. The FFT is faster than the DFT by a factor of 340, 190, 100, and 60 for record lengths that are 4K, 2K, 1K, and 0.5 K respectively. The dramatic difference derives from the degeneracy (gross repetition of calculations) that is part of the DFT. One can appreciate the improved efficiency by considering a pedagogical case with only 8 samples, rather than the minimum of 1024 for any programs of this document. The transform involves roots of unity in the complex plane, as noted in [R. Peters, “Fourier Transform construction by vector graphics”, Am. J. Phys. 60 (5), 439 (1992)]; i.e., the unit vectors shown in Fig. 22.

To obtain the transform, multiple rotations around the unit vector circle are required, as in the DFT (upper) case. Cooley and Tukey figured out how to permute the indices of the binary numbers representing the vectors, so as to reduce the computational overhead dramatically. Consider the following sequence of 8 numbers: (000), (001), (010), (111). If the least significant bit is the farthest right, then the sequence shown is 0, 1, 2,, 7. On the other hand, if the least significant bit is on the left instead, then the sequence is 0, 4, 2, 6, 1, 5, 3, and 7 (as shown in the FFT (lower) case). This bit reversal scheme permits all vector components to be determined once only. With the DFT, the components are calculated over, and over, and over, and unnecessarily. Of course, at the end of FFT computation, the answer must be “unscrambled” from the coding.

[NOTE: Do not attempt to operate GSM program #26 with inputs that are not integer multiples of K, where K = 1024. The program is only configured to accommodate records for which $N = 2^n$,

where n is integer.]

An example of output from PSM program (6) is provided in Fig. 23a (time record). Its power spectrum, using GSM program #26 is shown in Fig. 23b. The 3rd, 5th, and 7th harmonics of the distorted (though periodic) velocity graph are readily visible.

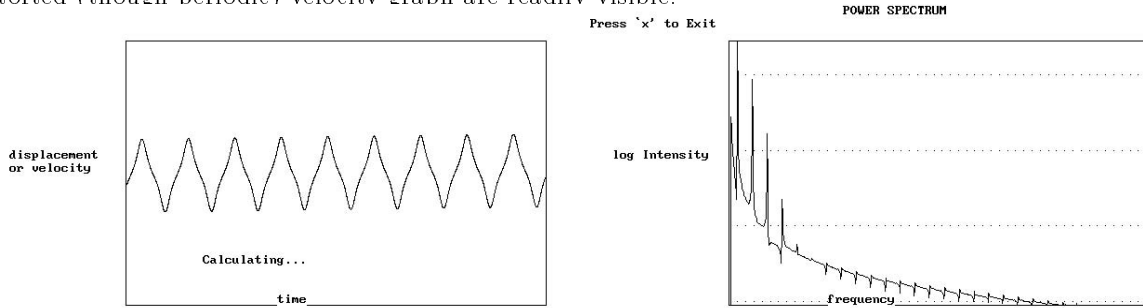


Figure 23: Simulation of the bell ringer pendulum mode using PSM pgm. #6.

(a). Time record of the velocity

(b). Power spectrum of (a) from GSM pgm.

#26.

SOME RECOMMENDED EXERCISES (EXPERIMENTAL)

The TEL-Atomic MPCP is interfaced to the computer through the serial port. Serial ports, in general, are much slower than parallel ones; but for the MPCP this is not a serious problem. The 50 Hz sample rate for the 2 channels is adequate, because the period of the pendulum is rather long. What is a bigger problem has to do with the rate at which the monitor can be updated with graphical information. Although the 286 Intel (old IBM-XT) can be used with the pendulum, it is preferable to work with at least a 386 or 486 (or even Pentium) machine. The reason is that the curves plotted (“Line” call within QBasic) are smoother (within the 50 Hz serial restrictions), the faster the CPU.

Some useful exercises are the following:

- (A) Free Decay: (1) Observe that the position and velocity are essentially 90 degrees out of phase with each other at low levels.
- (2) Notice that the log decrement is different, depending on the moment of inertia of the pendulum.
- (B) Driven Motions: For a variety of pendulum configurations and drive frequency and amplitude cases, look at the time records. Can you find any apparently chaotic cases?

PHASE TRAJECTORIES

- (1) For a free decay, look at the logarithmic spiral. (The best way to establish this curve is to let the pendulum come to steady state and then flip the switch that turns the drive off to the pendulum.) See how the rate at which it approaches the origin is different, depending on the moment of inertia of the pendulum. Do you see any connection between this graph and the earlier time demonstration of free decay? (2) For a variety of configurations similar to the earlier cases (time representation) look at the phase trajectories. What happens when the motion is chaotic?

POINCARÉ’ SECTIONS

Before Poincaré’ sections can be generated, it is necessary that the appropriately labeled switch be thrown.

- (1) Set up a periodic motion and observe the finite number of points, depending on the order of the so-called “limit-cycle”. (2) Set up a chaotic case and observe the development of a fractal. Note: Instead of the usual strobed phase space, the one being used by the program is based on the embedding theorem. It plots the present value of the pendulum’s velocity against the velocity one drive cycle earlier. This is easier to implement. The geometries are not the same. For one interested in the more common case, refer to the earlier discussion under “phase space”.

PENDULUM PARAMETERS

Any meaningful comparison of your pendulum directly with computer simulations requires that the parameters of your system be known. A parameter that is readily determined is the motor torque as a function of rheostat setting. It is recommended that this be done for at least two settings.

(1) Measure the motor torque for two significantly different settings on the drive amplitude scale, such as (i) 50 and (ii) 100 .

One way to do this is to measure the masses of both (i) the rod, and (ii) the bob. Then, for static deflection of the bob, measure the angle with respect to vertical. The torque is then readily calculated using elementary principles. (The static deflection is measured using position 1 of the frequency selector switch.)

Another necessary data set involves the drive frequencies. These can be readily determined by using a stopwatch. A useful means, for a given setting, is to measure the time required to complete ten cycles of the drive (20 clicks of the relay) and then divide your measurement by 10.

(2) Measure the frequencies of the drive motor for the switch settings available.

(3) (a) Measure the log decrement of the pendulum's motion in free decay, for two different (measured) placements of the bob on the rod. Be sure and also measure the frequency of the pendulum for each of these bob positions. (b) Calculate (i) the total moment of inertia of the pendulum and (ii) c using Eq. 2, section 2.3. How much of I 's value is due to contributions other than from the rod and bob? In particular, estimate the moment of inertia of the motor armature after subtracting contributions from: (i) the bob (ii) the rod, and (iii) the aluminum disk. Estimate the disk's mass using the density for Al and a rough measurement of its volume.

RESONANCE STUDY

In these exercises, you will tune from high to low frequency of the drive torque, keeping the torque constant for a given resonance response.

The numbers specifying "settings" in the discussion to follow are with respect to the scale on the rheostat which controls the torque.

After each frequency change, you must wait for the transient to die out. Then measure the peak amplitude of the motion (time representation) or the long dimension of the phase space "ellipse".

After obtaining the amplitude vs frequency values, for a given drive, plot the data on graph paper. For low drive, this will be the classical Lorentzian.

For a pendulum length (center of bob to axis) of 10 cm, generate a resonance curve for each of the following settings of the rheostat: (a) 0 (b) 25 (c) 50 (d) 100.

Thus you will graph four different cases. As the drive gets larger, the Lorentzian will become increasingly distorted. Does the distortion (according to literature terminology) correspond to "hardening" or "softening" of the system?

In the final case, the motion will probably go chaotic at some frequency. Identify the frequency at which this happens. By trial and error in the rheostat setting, you should be able to establish a bell ringer motion by tuning downward as in the resonance study. Identify the setting and collect records for FFT analysis. Compare with PSM program #6 output.

5 PETERS AUTOMATED PENDULA (PAPA)

TABLE I: PAPA ¹

- | | |
|-----------------------------------|--|
| 1. Precision Simple Pendulum | 2. Conical Pendulum |
| 3. Adjustable Trends Pendulum | 4. Kalman Filtered Pendulum |
| 5. Support Constrained Pendulum | 6. Ink-jet Pendulum |
| 7. Cavendish Balance (Pendulum) | 8. Long Period Physical Pendulum |
| 9. Tilt Sensitive Pendulum | 10. Modified Analytic Balance (Pendulum) |
| 11. Leaky Pendulum | 12. Torsion-gravity Pendulum |
| 13. Multipurpose Chaotic Pendulum | 14. Servo-controlled Pendulum |

One reason for providing the present document is to solicit feedback from purchasers of existing equipment concerning additional instruments they would like to see developed from the PAPA group. Some instruments, such as the ink-jet pendulum, could be available for purchase rather quickly; whereas others, such as a pendulum with adjustable trends in the period, would require more extensive development.

Through the years some people have questioned whether a given instrument should be referred to as a balance or as a pendulum. For example, depending on the author, the same torsion instrument has at various times been described by both terms. Either term is acceptable; since unless damping is severe, a balance will oscillate after being disturbed. For the present document, the word “pendulum” is being used in a generic sense to describe a host of different mechanical oscillators.

Some of the above innovations are improvements on old themes by means of automation. They combine modern high technology with concepts that go back 300 years to the time of Galileo. Other innovations represent altogether new types of mechanical oscillators. By automated is meant that the computer is used for studying the motion, controlling the motion, or measuring some property, such as the period of the pendulum. Interestingly, a referee dealing with a paper on the Cavendish balance indicated that “it’s impossible to “improve” the balance that Cavendish built”. What this individual failed to realize is that Cavendish didn’t do it the way most people have seen it, with an optical lever; rather he directly viewed the swinging masses with a telescope. Cavendish most likely would have preferred the automated approach to this measurement.

5.1 Precision Simple Pendulum

In the first case from Table I of a simple pendulum, which comprises a small metal bob on a flexible wire, the computer was used in real time to graphically display the period of the large amplitude motion as a function of amplitude during free decay[B1] . This was one of several exercises that were part of a computational physics course in which colleague Tom Gibson taught the lecture part of the lecture/lab course. The laboratory goal of this course was to introduce students to operational features of data acquisition and processing using a personal computer. Many students in recent years have been “connected” to an experiment with a PC, but the objectives of this lab were different. In particular, familiarization with generic features of digital computing was deemed necessary; i.e., at least an introduction to operations at the machine code instruction level. This could be done with virtually any machine, but the one chosen was the very inexpensive Radio Shack Color Computer II (CCII), which is no longer manufactured. Many have jokingly referred to the Radio Shack computers as “trash” systems; however, for the time, the architecture of the Motorola hardware in the CCII was outstanding. In the laboratory studies, the CPU processor was itself used to measure both the period and amplitude of the pendulum. This was done with a standard photogate circuit (air track type) connected to one of the several user ports of the computer as illustrated in Fig. 24.

This scheme is commonly employed today, by commercial systems that provide the “pendulum time” as well as more traditional interval measurements. In this approach an assembly language generated

¹Currently, only two pendula are available from the PAPA group: (i) the multipurpose chaotic pendulum and (ii) the Cavendish balance. Peters’ three granddaughters call him Papa Rose, since circumstantially, Mama Rose (his wife Rosalee) was the first grandparent they knew.

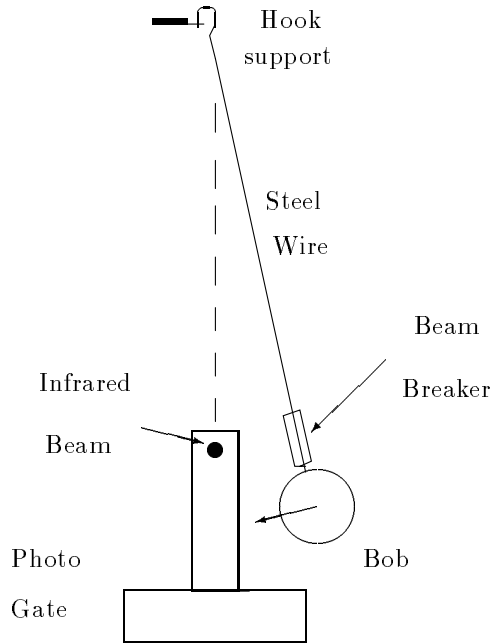


Figure 24: Example simple pendulum suitable for automation.

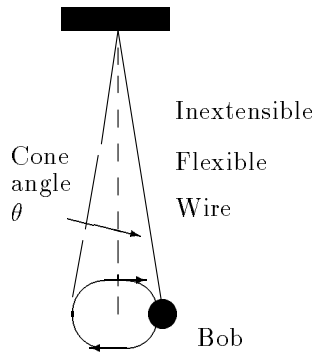


Figure 25: Motion of a Conical Pendulum.

program was used to measure two time intervals [B1]. These were (i) the duration of photogate beam interrupt by the bob (related functionally to the amplitude), and (ii) the cycle repeat time of the pendulum. By assuming that the peak velocity (bottom of the swing) is proportional to the amplitude, the computer was used to calculate the amplitude. The CPU clock frequency was high enough (low MHz) to give accuracies for the period in the tens of parts per million. Thus the variation of period with amplitude could be readily demonstrated. Also, a favorite student exercise was to watch the period change as the stranded steel support wire was heated with a torch, and thereby lengthened by thermal expansion. One has to be careful, of course, not to burn the wire in two. An invited talk dealing with some of these techniques was well received at the 2nd national conference and workshop on computing in undergraduate education held in Asheville, N.C. in 1989.

5.2 Conical Pendulum

An interesting pendulum that is not well known, at least in terms of the variation of its period with cone angle, is the conical pendulum, illustrated in Fig. 25.

Rather than motion in a plane as with the standard planar pendulum, the bob in this case moves

through the photogate once per cycle, the trajectory being a circle. Fowles [B2] deals with the conical pendulum, and also analyses the case when the trajectory deviates slightly from a circle. Using elementary theoretical considerations, it is easy to show that the period of a conical pendulum does not lengthen for increasing angle as a planar pendulum does for increasing amplitude. Instead, the variation is oppositely directed; it shortens at larger angle according to the following expression:

$$T = 2\pi \sqrt{\frac{L \cos\theta}{g}} \quad (8)$$

Students may readily (without calculus) derive this equation, by considering the centripetal force on the bob; which is given by $F \sin\theta$, where F is the tension in the string.

To compare with the better known case, we use the following well known approximation for the planar pendulum:

$$T \approx 2\pi \sqrt{\frac{L}{g}} (1 + A^2/16) \quad (9)$$

This expression represents the 1st order correction to the period at infinitesimal amplitude. Expanding the cosine term to the same order, we see that the effect of finite amplitude on the conical pendulum is to shorten the period by $\theta^2/4$. Conversely, the planar pendulum with amplitude $A = \theta$, experiences lengthening by $\theta^2/16$. Thus the conical pendulum is 4 times more sensitive to the amplitude, as well as trending in the opposite direction. These differences were easily demonstrated with the photogate based apparatus.

5.3 Adjustable Trends Pendulum

A second automated simple pendulum was one which also used a photogate; however, for timing, a precision (Hewlett-Packard) period counter was employed [B3], so that measurements in the low parts per million range could be performed. Additionally, this permitted the computer to be available for estimations of the period using optimization theory (Kalman filtering), as mentioned later. The interface to the HP counter was one which used the binary coded decimal (BCD) data that was part of the counter's hardware architecture. The results of student John Shepherd's work on this interface were published [B4].

One of the payoffs from John's work was the possibility to make new types of measurements on a precision pendulum operating in vacuum. The earliest similar study was probably that of J. C. Maxwell who, with a coworker in the 1800's, placed a pendulum in vacuum to see what the influence on damping would be. Maxwell was led to this experiment because he had predicted, according to the kinetic theory of gases, that the dissipation would be essentially unchanged until the pressure got quite low. His prediction proved correct.

In a manner that is characteristic of many discoveries by serendipity, an interesting trend in the period was found when the precision pendulum was placed in vacuum. To eliminate problems of vibration, the mechanical pump was turned off after reaching a pressure level corresponding to tens of microns of Hg. Because of a small leak in the chamber, this gave rise to a steady increase in pressure and consequently a surprising result. The initial amplitude of the freely decaying pendulum was large enough to significantly increase the period. Thus there were two competing trends present. First, through decay, there was a component causing period decrease with time, due to the effect of finite amplitude. Second, because of buoyancy (and added mass effects [B5]), the period experienced a lengthening component, because of the pressure increase. It has been said that Newton showed that inertial mass and gravitational mass were equal to a part per thousand, using the pendulum. This experiment points out that buoyancy and added mass effects disallow equality to better than a ppm unless the vacuum is excellent.

It was found that control of the trend was possible, for a given leak rate, depending on the amplitude of the initial motion. Normally at large amplitudes a simple pendulum is not isochronous; i.e., the period is not the same for all amplitudes. In the case cited, because of the opposing trends, it was possible to select an initial operating amplitude for which isochronism was possible (to a few ppm) for a time interval of several minutes.

5.4 Kalman Filtered Pendulum

In the world of applied physics and engineering, a powerful estimation tool became popular in the 1960's. The tool is commonly known among engineers but not physicists. This optimal estimation computational technique has become associated with the name, Kalman. Using the techniques of Hamiltonian mechanics (in matrix form), it factors both measurements and theoretical knowledge of the state equations of a system into the estimates that are generated. The algorithm is iterative, and the confidence in its prediction increases with time, if prerequisites for proper development are met. Qualitatively, the algorithm works in the following way. At the time of initialization, the measurements dominate the estimate. As time progresses, they become de-weighted as more and more weight is placed on the theoretical prediction concerning state variable evolution. Such algorithms were used in the development of various parts of the fire control system of the AH-1S Cobra Helicopter. During this time it became clear that the simple pendulum represents an excellent pedagogy for understanding Kalman filtering [B6]. Moreover, it enables the pendulum to perform its traditional task in a better way; i.e., to measure the acceleration of gravity more quickly and accurately. Historically, in an attempt to eliminate errors resulting from the amplitude dependent period, the pendulum has been operated in the milliradian range [B7]. This method for reducing what has usually been considered a systematic error has the disadvantage that there are accompanying increased random errors. By accounting for the amplitude dependence in the filter, and operating at larger amplitudes than normal (up to several degrees); it is possible to estimate the zero-amplitude value with higher precision and in less time. Of course this method was not possible before the computer.

The solution is based on the following assumptions— first that the period depends on the amplitude in the following manner,

$$T = T_0 \left(1 + \frac{\theta_0^2}{16} \right) \quad (10)$$

where θ_0 is the amplitude in radians. The second approximation is that the decay of the amplitude is described by a single exponential,

$$\theta_0 = \theta_{00} e^{-\alpha t} \quad (11)$$

This assumption has been found to be acceptable [B6] when the total time of measurements does not exceed 10 minutes.

These two assumptions permit simple equations relating the measurement, the estimates of period and period rate, and their variances. The first step is to combine equations (10) and (11) to yield

$$T = T_0 \left(1 + \frac{\theta_{00}^2 e^{-2\alpha t}}{16} \right) \quad (12)$$

Thus the period and its first derivative are related by

$$T_0 = T + \frac{\dot{T}\Delta}{2}, \quad \Delta = 1/\alpha \quad (13)$$

Thus it is seen, for known Δ , that estimates of period, T , and period rate, \dot{T} , at a finite amplitude (less than 5 degrees typically), permit an estimate of the zero-amplitude period T_0 , which is related to the acceleration of gravity and the pendulum length in the well known manner,

$$T_0 = 2\pi \sqrt{\frac{L}{g}} \quad (14)$$

Since the estimation process provides both the period and its rate at every update time, the zero-amplitude period can be estimated at each of those times without computing the amplitudes. This technique is discussed further in Appendix III.

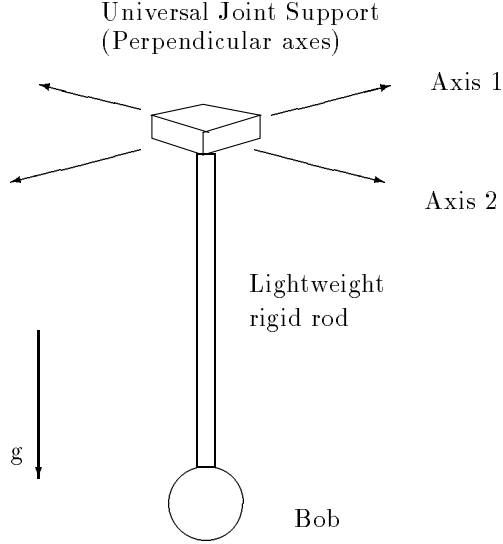


Figure 26: Support Constrained Rigid Spherical Pendulum.

5.5 Support Constrained Pendulum

In the original instrument built by John Shepherd, a bowling ball was suspended from a universal joint with a section of pipe. The pendulum is illustrated in Fig. 26.

The equations of motion for this pendulum are the following (in the absence of dissipation):

$$\frac{d^2\theta_1}{dt^2} \cos\theta_2 - 2 \frac{d\theta_1}{dt} \frac{d\theta_2}{dt} \sin\theta_2 + \frac{mgL}{I_1} \sin\theta_1 = 0 \quad (15)$$

$$\frac{d^2\theta_2}{dt^2} + \left(\frac{d\theta_1}{dt}\right)^2 \frac{I_1 \sin\theta_2 \cos\theta_2}{I_2} + \frac{mgL}{I_2} \cos\theta_1 \sin\theta_2 = 0 \quad (16)$$

where I_1 and I_2 are the moments of inertia in each of the two axes, m is the mass of the pendulum, and L is the distance from the center of gravity to the support. It can be readily seen that these reduce to two independent (orthogonal) simple harmonic oscillations, in the limit of small motion in both axes; i.e., the equations of motion become:

$$\ddot{\theta}_1 + \omega_1^2 \theta_1 = 0 \quad (17)$$

$$\ddot{\theta}_2 + \omega_2^2 \theta_2 = 0 \quad (18)$$

The resulting trajectories, corresponding essentially to the simple spherical pendulum, are well known and of little interest as compared to the wealth of complexity that results when the motion is large.

The motion in each of the perpendicular axes was measured with a capacitive rotary sensor. At low levels the system was found to produce Lissajous figures as expected. At larger levels, however, nonlinear terms in the Hamiltonian (primarily the velocity ones) give rise to fascinating motions. It was shown, through modeling, that the pendulum can be chaotic in the limit of zero damping [B8]. Even the system with damping shows sensitive dependence on initial conditions, and the figures that were generated with an x-y recorder connected to the two sensors represent a beautiful artform. In all cases they possess an inversion symmetry about the origin. Unlike the traditional spherical pendulum, the precession can reverse directions and give rise to a virtual infinity of different traces.

The simulation of this system [B8] did not use equations (15) and (16), since (as has been earlier noted) the accuracy would suffer. Instead, the equivalent set of four coupled 1st order equations was integrated [the routine being that used by GSM program #30]. The equations used in the simulation are provided in part II of this monograph.

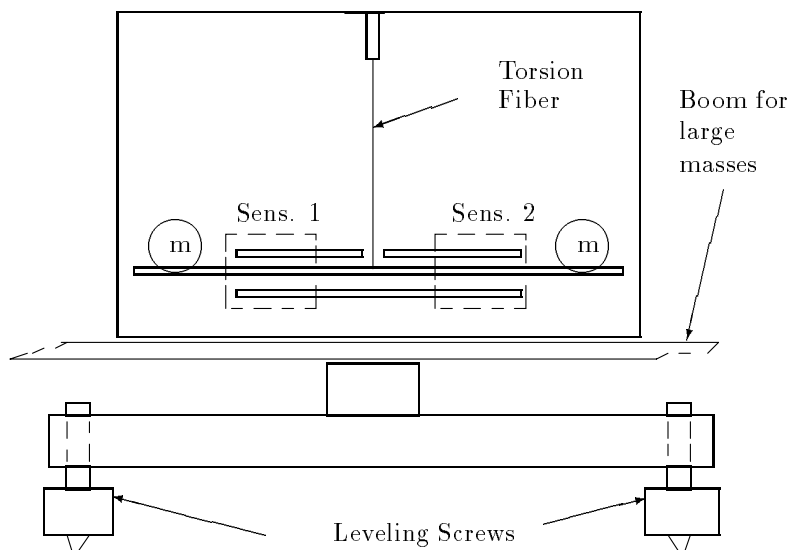


Figure 27: Cavendish Balance outfitted with two SDC sensors.

5.6 Ink-jet Pendulum

The primary difficulty with the original support constrained pendulum was the need for two separate sensors [B9] (and associated electronics) as well as an x-y recorder to generate trajectories. Now one can find brass and oak versions of this pendulum in gift shops—the motion of the brass pointer is recorded in “sand”. (Perhaps the toy manufacturer read the article in *Physical Review* where this pendulum was first published!) The most elegant way to record the motion is to connect an ink-jet impactless timer to the bottom of the pendulum. Available from IJIT Inc. (215 Fox Run, Huntington, CT., 06484) this instrument uses the ink dispenser from a Hewlett Packard deskjet printer. With the IJIT, not only do the beauties of the pendulum’s complicated motion get recorded, but there are the additional features of a Moire type. These result because of the 100 Hz dispensing rate of the ink microspheres. When the pendulum velocity is large, the separation between dots of the pattern is great, and vice versa for low velocity. Especially because of the reversals in precession that occur during decay, the Moire features look almost self-similar, except that they are more regular than chaotic. A planned future project is to use the support constrained pendulum in conjunction with a color inkjet dispenser. Ideally, one would like to be able to turn on or off any combination of the primary (subtractive) colors at any time during the motion of the pendulum.

5.7 Cavendish Balance (Pendulum)

After developing the first sensor of a new technology called symmetric differential capacitive (SDC), it was realized that this technology had the potential for revolutionizing small measurements on mechanical systems. One of its first applications was to the experiment first performed by Henry Cavendish in 1798. The TEL-Atomic product is illustrated in Fig. 27.

Many students have cursed the Cavendish apparatus in the form sold by Leybold. The biggest problem with this apparatus is its extreme sensitivity to vibrations. The second biggest is the tediousness that derives from manual recording of data (such as recording turning points of the motion). Both of these are avoided with the TEL-Atomic computerized Cavendish balance; and moreover, the SDC transducer (2 sensors) is more sensitive than a standard optical lever.

This Cavendish instrument is a dramatic improvement with regard to environmental vibrations. It has been routinely used on folding tables at conferences. Its increased immunity results from two features: the use of (i) a shortened support fiber, and (ii) two SDC sensors connected in electrical anti-parallel. There is an interesting story behind the long fiber of the Leybold system, which is a

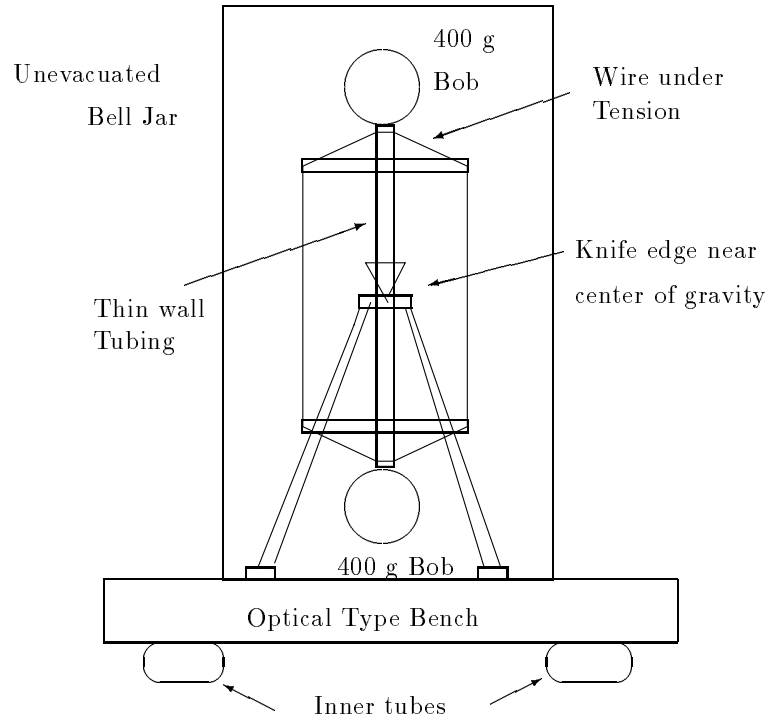


Figure 28: Long Period Pendulum for Mesodynamic Studies.

ribbon (rectangular section) rather than a wire with circular cross section. A ribbon may have some stability advantages; however, it is nonlinear, and especially so at large angles of twist. The ribbon length was chosen so that, for nominal deflections, the range of twist would stay within a reasonably linear region—thus the long support fiber. The nonlinearity is removed when a fiber with a circular cross section is used. In fact, such a torsion wire is one of the best candidates for obeying Hooke’s law, at large deflections. At very small deflections, it has been shown that anelasticity prevents most metals from obeying Hooke’s law. Many people think of nonlinear phenomena being important only at large levels; but they also become important at mesodynamic levels, because of anelasticity.

A short wire of small diameter has been used in the computerized Cavendish Balance. This is possible because the restoring constant of a circular wire is dependent on its diameter to the 4th power, whereas the length dependence (inversely) is only 1st power. For a given level of external noise, the amount of unwanted pendulous deflection increases with the length. Thus a significant immunity can be realized simply by shortening the fiber. The pair of SDC sensors provides substantial additional immunity, which is possible because the torsion mode is differential, whereas the pendulous one is “common”. Finally, the addition of a computer enables the experimenter to do things that just are not feasible apart from automation. This is especially useful for the Cavendish system because it is not possible to do a meaningful experiment in less than the better part of an hour. The sensitivity of a balance to external forces is proportional to the square of its period. Since the gravitational force is so weak, a long period balance is therefore necessary. By increasing the sensitivity of the detector, it is possible to operate with somewhat reduced periods. For example, in the past, 6-10 min periods were typical for the Leybold system. The computerized Cavendish balance functions very well when its period is in the range of 2-5 min.

5.8 Long Period Pendulum

This vertically oriented instrument is one in which the two spherical masses that constitute most of the mass of the pendulum are situated above and below the horizontal axis of rotation as shown in Fig. 28 [B10].

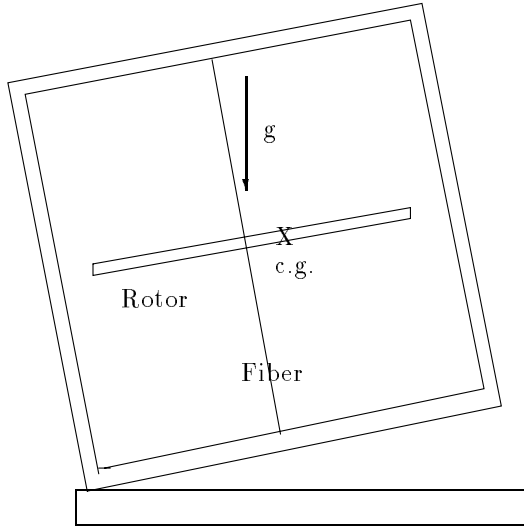


Figure 29: Tilt Sensitive Pendulum.

The center of gravity of the pendulum is vertically adjustable and located just micrometers below the axis, so that the period of the pendulum is quite long. At low levels it exhibits metastable states that are not associated with the supporting axis (a knife-edge or flexure strip). The attenuation of the motion (determined by internal friction of the material of the pendulum's structure) is of a type that had not been seen prior to the development of this pendulum. This instrument is of current interest because of the attention being given to the detection of gravitons. Mesoanelastic complexity is expected to place a limit on the sensitivity of these instruments.

5.9 Tilt Sensitive Pendulum

This instrument is a balance whose sensitivity is mechanically adjustable, as well as being a tiltmeter [B11]. At the heart of the instrument is a torsion wire, but it is different than the standard torsion pendulum. In the standard instrument, the fiber hangs along the direction of local vertical, with the torsion boom connected to the bottom of the fiber, which is tied at the top. In the tilt sensitive pendulum, the torsion fiber is secured at both top and bottom with the boom usually at the middle as illustrated in Fig. 29.

Because the center of mass of the boom will inevitably be located at a different place than the fiber (perhaps only microns), the instrument is tilt sensitive. Consider a primary tilt which places the c.m. either above or below the fiber. There are two components to the potential energy of the instrument: (i) the nearly Hookean twist of the fiber, and (ii) the acceleration of gravity. If the c.m. is placed, due to tilt, below the fiber; then the system is "hardened" and the sensitivity less than what would be true in the absence of gravity. On the other hand, if the c.m. is placed above the fiber, the two potential components work in opposition to each other; so that the sensitivity is increased. Because gravity is trying to pull the bob to below the fiber, and torsion is trying to keep it above, the net potential energy is one that can be quite shallow. A shallow well gives rise to a long period instrument that is very sensitive, since the sensitivity is proportional to the square of the period. The pendulum is very effective in a variety of capacities. It can be made to function, for example as an adjustable balance for force measurements at low levels, or as a sensitive tiltmeter. A tilt at right angles to the earlier described primary tilt causes the moving member of the instrument to rotate through a much larger angle than the amount of secondary tilt; i.e., there is a significant mechanical amplification. As the tilt increases, however, a critical point may be reached (for a sufficiently weak fiber), beyond which the system becomes unstable. Physicists who are familiar with the work of the Compton brothers will recognize in this operating principle some similarities to their electrometer. This instrument is described in the "bible" of experimental physics by John Strong [B12].

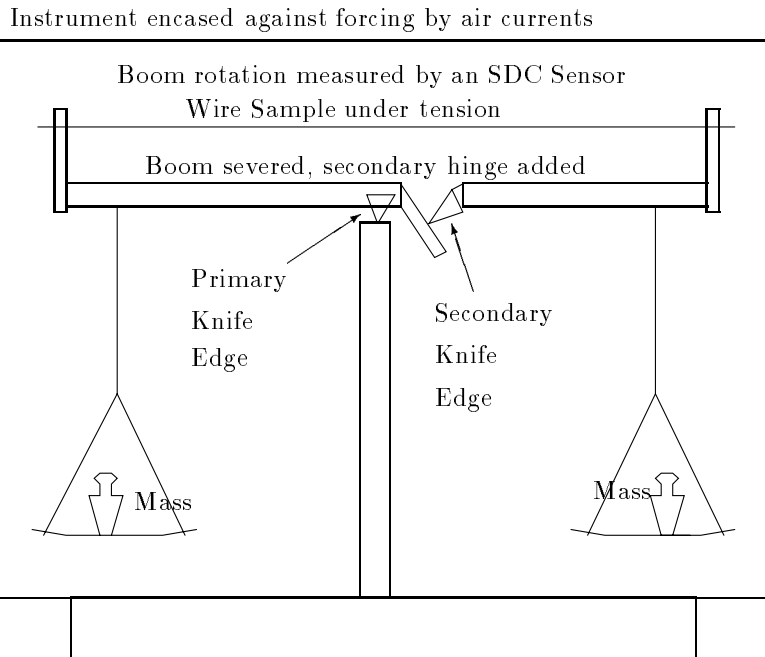


Figure 30: Modified Analytic Balance Pendulum.

5.10 Modified Analytic Balance (Pendulum)

The old-style chemical analytic pan balance for measuring mass, which was so common in previous years, is a type of pendulum. The period, and thus the sensitivity of the instrument, is adjustable according to the vertical position of a small mass that rides on the pointer rod. The modified analytic balance is one that grew out of concern for alternative methods to study anelasticity. The word, anelasticity, is as used by Zener [B13] to describe the real properties of materials, such as metals. In real, as opposed to idealized materials, Hooke's law is not obeyed because the atoms engage in "musical chairs" during creep. The modification is one in which the main boom of the instrument was severed just to the side of the primary knife edge as shown in Fig. 30.

A secondary hinge was added at this point along with outrigger posts on the ends of the primary boom. In turn, the sample of wire selected for study, is tied to the outriggers. This sample, under tension, is all that keeps the system from collapsing about the secondary hinge. Why build such an instrument? Because as the instrument oscillates, there is a low level periodic stress in the sample. Additionally, the amount of mass on the pans determines the mean value of the stress in the sample. The device has been useful for studying mesoanelastic complexity.

5.11 Leaky Pendulum

The idea for this pendulum originated with Ray Mires of Texas Tech University, who was familiar with a problem of related type in a popular physics textbook [B14]. The construction and first attempts to study a leaky pendulum were those by a graduate student under Ray's direction at TTU. A potentiometer was used as a position sensor in the first version of the pendulum, which was fabricated from PVC tubing. These efforts were mainly unsuccessful for a variety of reasons, not the least of which was friction in the potentiometer. A later instrument using an LRDC sensor proved better, but the noises in the system were severe. This resulted because of an improper operation of the sensor by two other students. The project was revived by doctoral student Virgil Jackson, who obtained excellent results using both water and alcohol in the instrument. Later, the "loose ends" of this work were "wrapped up" by completing the experiments and also by doing the first derivation of every equation in the published paper [B15]. The leaky pendulum is illustrated in Fig. 31.

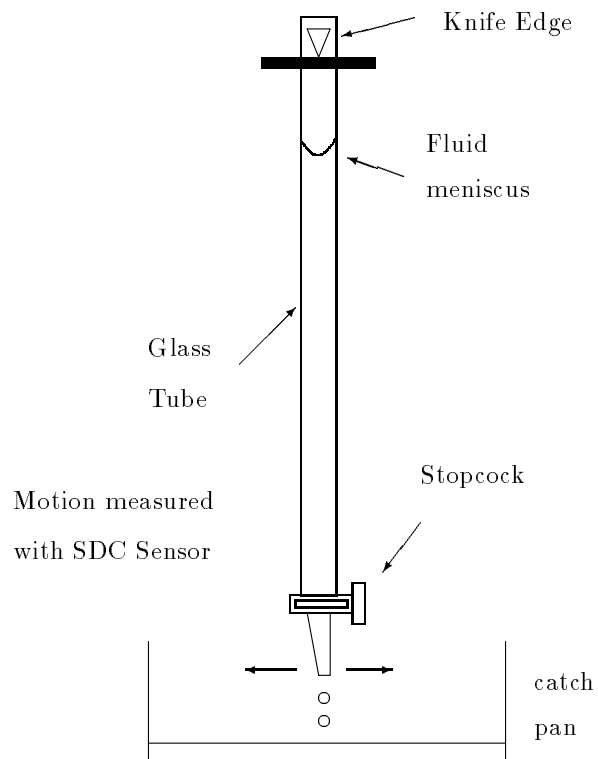


Figure 31: Illustration of the Leaky Pendulum.

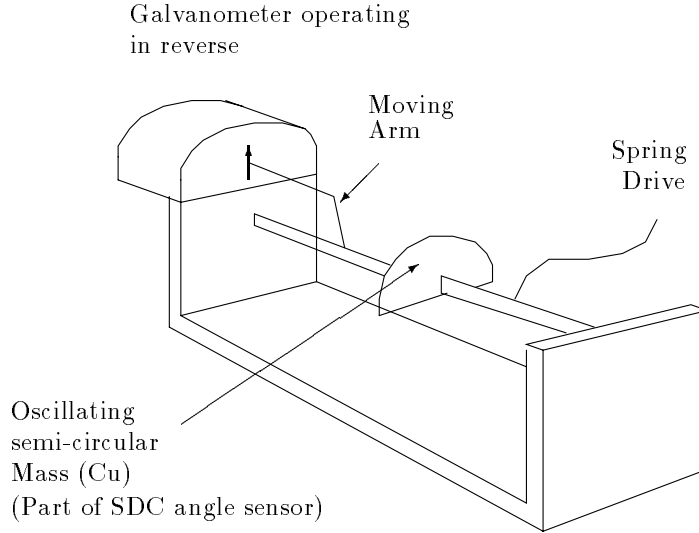


Figure 32: Torsion-Gravity Pendulum.

5.12 Torsion Gravity Pendulum

This pendulum is one in which typically the forces of torsion and gravity act in opposition. It is illustrated in Fig. 32.

It is similar to the mechanically adjustable tilt meter, except that it operates beyond the critical point. Consequently the pendulum is a two-well oscillator; which reduces for narrow separations of the wells, to the Duffing case. *It is not the Duffing system that is well known for amplitude jumps and hysteresis—one term in the equation has the opposite algebraic sign.* The vertical position of the bob is an unstable equilibrium point, and the wells are located on each side of vertical. By using a ribbon torsion element, the well separation distance can be adjusted by altering tension in the ribbon. If the drive becomes very large, the system becomes multi-well as the bob participates in “winding” (multiple passages through vertical). Then the potential departs from the Duffing approximation and becomes a “modulated” parabola. It is characterized by “trapping states”. This particular form allowed the discovery of a new map [B16], which looks similar to the Chirikov map. The Chirikov map is essentially a description of the pendulum in iterative as opposed to differential equation form. It is important because the pendulum has been recognized as the paradigm of nonlinear physics; just as the simple harmonic oscillator (SHO) is the paradigm of linear physics. The Peters map is interesting in the following respect. For small values of its adjustable parameter, the pair of equations reduce to the SHO. For intermediate values it reduces to the Duffing oscillator. For large values it reduces to the pendulum. Thus it is capable of representing several significant systems. For more information on this pendulum, see appendix II.

5.13 Multi-Purpose Chaotic Pendulum

The Multi-Purpose Chaotic Pendulum (planar), marketed by TEL-Atomic is an apparatus of considerable pedagogical diversity, and was the first “honest to gosh” pendulum to be sold commercially by the company. If the use of “pendulum” with the classic “G” measuring instrument is allowed, then the computerized Cavendish balance was the first commercial instrument offered by TEL-Atomic. Among the PAPA entries in Table I, the precision instrument and the multi-purpose instrument are the only “true” pendula as known for centuries to the physics community. The multipurpose instrument was originally intended solely for studying the new science of chaos; but shortly after the first prototype was built, it was discovered that the apparatus is useful to the study of mechanics in a large number of

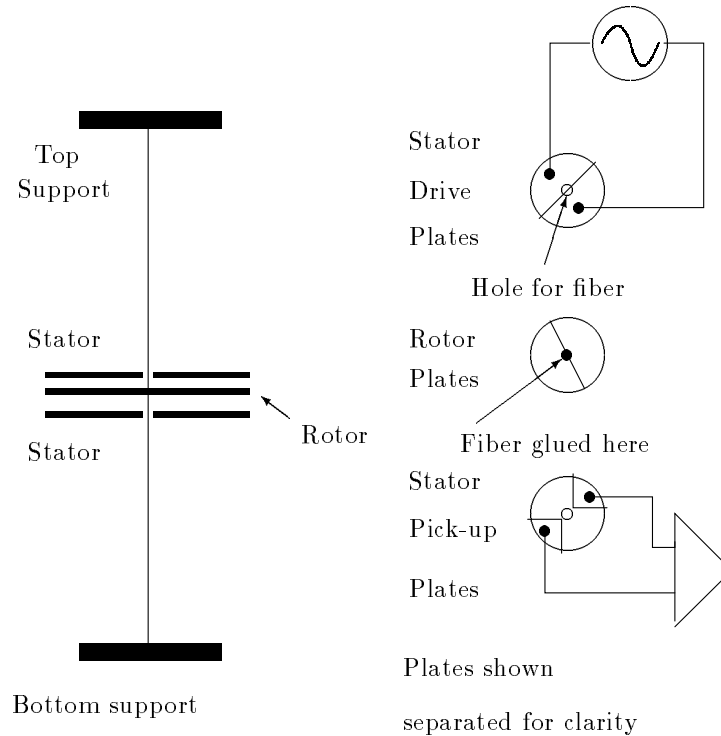


Figure 33: Illustration of an LRDC Transducer.

areas. Additionally, it has even demonstrated a phenomenon which was previously only well known to European bell-ringers who have “rung up the bell”. This phenomenon, which does not involve chaotic motion, is concerned with the resonance response of a rigid planar pendulum, driven at large amplitudes, but not enough to go past vertical. It illustrates, once again, the inappropriateness of the term “simple” pendulum. Only the models used to describe the pendulum (within limited realms of acceptability) are truly simple.

5.14 Servo Controlled Balance (Pendulum)

The SDC sensors can function as actuators in those cases where the variation of capacitance is by means of area change. The device is configured so as to have two different equilibria—one associated with a restoration derived from mechanical means and the other restoration coming from the transducer itself. The earliest SDC transducer was one which went by the name linear rotary differential capacitance (LRDC). The configuration used for the servo studies was one with no mechanical contact, shown in Fig. 33, used to measure rotor twist of a small diameter tungsten wire.

Obviously this scheme can succeed only when working with a very weak mechanical part, since the restoring force derived from the capacitive part is very weak. Such an instrument was built using a tungsten wire whose diameter was $25 \mu m$ [B17]. The sensor was made to operate simultaneously in both the sense and actuate modes as shown in Fig. 34.

This was possible because the sense function depends on exciter voltage to the first power, whereas the actuator function is proportional to the same voltage to the second power. The servo loop was rather conventional, except that the system is nonlinear. It was possible to model its essential features with the computer.

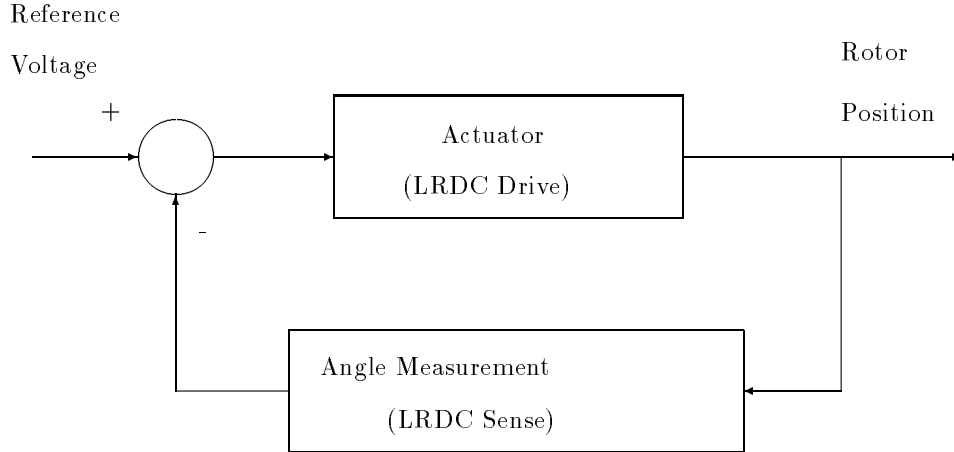


Figure 34: Block Diagram of a servo-controlled pendulum.

REFERENCES (PAPA)

- (B1) R. Peters, "Experimental computational physics using an inexpensive microcomputer", *Comp. Phys.* 2 (4), 68 (1988).
- (B2) G. Fowles, *Analytical Mechanics*, 2nd Ed., Holt, Rinehart & Winston, p. 111 (1970).
- (B3) R. Peters & J. Shepherd, "A pendulum with adjustable trends in the period", *Amer. J. Phys.* 57 (6), 535 (1989).
- (B4) J. Shepherd, "An inexpensive BCD counter interface for the TRS-80 Color Computer II", *Undergrad. Res. in phys.* 6 (2), 39 (1988).
- (B5) R. Nelson & M. Olsson, *Am. J. Phys.* 54 (112) (1986).
- (B6) R. Peters, "Period estimate for the simple pendulum using optimization theory", *Appl Math. and Comp.* 28 (3), 179 (1988).
- (B7) P. Heyl & G. Cook, *J. Res. Nat. Bur. Standards* 17, 805 (1936).
- (B8) R. Peters, "Chaotic motion from support constraints of a non-driven rigid spherical pendulum", *Phys. Rev. A* 38 (10), 5352 (1988).
- (B9) R. Peters, "Linear rotary differential capacitance transducer", *Rev. Sci. Instr.* 60 (8), 2789 (1989). U. S. Patent No. 5,028,875.
- (B10) R. Peters, "Metastable states of a low frequency mesodynamic pendulum", *Appl. Phys. Lett.* 57, no. 17, 1825 (1990)
- (B11) R. Peters, "Mechanically adjustable balance and sensitive tilt meter", *Meas. Sci. & Tech.* 1 (11), 1131 (1990).
- (B12) John Strong, *Procedures in Experimental Physics*, Prentice Hall (1938).
- (B13) Clarence Zener, *Elasticity and Anelasticity of Metals*, Chicago Press (1948).
- (B14) R. Resnick & D. Halliday, *Physics, part I*, p. 375, Wiley, New York (1966).
- (B15) R. Mires & R. Peters, "Motion of a leaky pendulum", *Am. J. Phys.* 62 (2), 137 (1994).
- (B16) R. Peters, "Experimental Evidence for a new frontier", *Proc., 3rd conf. on complexity*, Minsk, Belarus (1994).
- (B17) R. Peters et. al, "Capacitive servo-device for microrobotic applications", *J. Micromech. Microeng.* 1 (103) (1991).

Index

- acceleration of gravity 38
- actuator 14, 46
- adjustable trends pendulum 37
- aluminum disk 13, 34
- amplitude jumps 10, 45
- analog 17
- analog to digital conversion 12, 35
- analytic balance pendulum 43
- Anderson, Philip 5
- anelasticity 3, 41, 43, 47
- angle measurement 20
- array 19
- artform 39
- asymmetry 9, 10, 14
- attenuation 16, 17
- BCD data 37
- bell ringer mode of the pendulum 11, 24, 34, 46
- bifurcation 8
- binary numbers 32
- bipolar 16
- Braginsky 14
- bridge 12, 14, 17, 20
- calibration 9
- cantilever 12
- capacitor 12
- capacitor force 14
- Cavendish 35, 40
- chaos 3, 4, 5, 6, 8, 10, 11, 24, 27, 30
- characterization 9
- CMRR 16
- coherence 15
- Chirikov 8, 11, 45
- compactness 17
- complexity 3, 5, 6, 7, 8, 9, 11, 24, 28, 39, 41, 45, 46
- Compton brothers 42
- computerized 8, 24, 40, 41, 45
- computerized pendulum 24
- conical pendulum 36
- control 12, 13, 14, 21, 23, 32, 34, 35, 37
- Cooley-Tukey 32
- creative 6
- Cromer-Euler 9
- CPU 36
- crucial invention 17, 20
- Daedalon 28
- damping 8, 10, 13, 24, 27, 35, 37, 39
- demodulator 14, 16, 17
- decibel 16
- defaults 24
- Dicke, Robert 14
- differential 3, 12, 16, 20, 40, 41, 46, 47
- digital systems 17
- drive 12, 26
- Duffing 8, 45
- dynamic range 12
- eddy currents 12
- edge effects 17
- electronics 22
- embedding 30
- equipotentials 17
- equivalence principle 37
- equivalent circuit 18
- estimation 87
- experimental 9, 33, 42, 47
- Fast Fourier transform 32, 34
- filter 15, 16, 35, 37
- Fowles 37
- fractal 7, 10, 30, 33
- frequency control 12
- friction 13, 43
- full bridge 20
- free decay 33
- Gleick 5, 6, 7
- grating 20
- Hamilton's method 27
- hardening 14, 34, 42
- hardware routines 26
- Hewlett-Packard 17
- hysteresis 3, 8, 9, 10, 45
- IJIT 40
- induction motor 12
- ink-jet pendulum 40
- interface 28
- instrumentation 6, 16, 17
- instrumentation amplifier 16, 19, 20
- integrator 12, 23, 28
- internal friction 3, 42
- inversion symmetry 39
- isochronism 37
- Joule heating 23
- Kalman filtered pendulum 38
- Laplace transform 24
- leaky pendulum 20, 43
- Leybold 40
- limit cycle 33
- linearity 15, 45
- linear position 19
- lock-in amplifier 15
- log decrement 8, 13, 24, 33
- logarithmic spiral 27
- long period pendulum 14, 35, 41

Lorentzian 24
 lower branch 10
 LRDC 21, 43, 46
 LVDT 16
 measurements 34
 mechanical amplification 42
 MEMS 16
 mesoanelastic complexity 6, 17, 42, 43
 mesodynamic 3, 41, 47
 metals 3, 5, 41, 43, 47
 metastable states 47
 Moire 40
 moment of inertia 8, 13, 33, 34, 39
 motor 8, 12
 multipurpose chaotic pendulum 45
 multiplication 15
 musical chairs (atoms) 43
 nonlinear 3, 5, 6, 8, 9, 11, 24, 28, 39, 41, 45, 46
 oak and brass pendulum 40
 optical methods 14, 20, 35, 40
 oscillators 6, 17, 35
 output reactance 17, 19
 PAPA 35
 paradigms 45
 patterns 6
 pendulum 6, 8, 9, 10, 11, 20, 24, 27, 28, 29, 30, 33, 35, 36, 37
 pendulum parameters 33
 pendulum simulation 25
 pendulum simulations menu 24
 pendulum trends 37
 period rate 38
 periodic boundary conditions 27
 permanent magnets 12
 phase 8, 10, 12, 15, 16, 17, 24
 phase noise 17
 phase perturbation 10
 phase space 27
 phase space trajectories 29
 planar pendulum 37
 Poincaré section 10, 12, 24, 26, 28, 33
 Portevin LaChetelier 5
 power spectra 30
 precession 39
 precision simple pendulum 35
 Princeton Applied Research (PAR) 17
 quantum 6
 QuickBasic 9, 25, 33
 ratio transformer 20
 reductionism 3, 5
 reference signal 15, 16
 relay 12
 resonance 8, 9, 10, 14, 24, 34, 46
 resonance study 34
 resonant circuit 14
 rheostat 13, 23, 34
 rotation 17
 sampling rate 33
 scanning tunneling microscope 17
 scaling 19
 Schaevitz 16
 sdc sensor 3, 6, 12, 13, 14, 16, 17, 18, 19, 20, 21, 40, 46
 self similarity 30
 sensitive dependence on initial conditions 10
 sensitivity 19, 20
 serendipity 21
 servo controlled balance 46
 Shepherd, John 37
 shielding 20
 signal to noise ratio 15, 16
 Signetics 16
 simple harmonic oscillator 24
 softening 9, 34
 software 24
 spherical pendulum 39
 spherical pendulum 39, 47
 square wave drive 12, 26
 steady state 8, 9, 10, 24, 27, 33
 stray capacitance 20
 strobing 30
 Strong John 47
 superposition 24
 support constrained pendulum 39
 symmetry 6, 12, 14, 16, 17, 20, 39
 synchronous detection 12
 Thevenin 19
 tilt sensitive pendulum 42
 time records 24
 timer 9, 21, 23, 40
 timer 40
 torsion gravity pendulum 45
 transformers 16
 transient chaos 10
 transients 10, 34
 trapping states 45
 tuning 10, 34
 universal joint 39
 unlimited range 21
 upper branch 10
 vacuum tube 17
 van der Pol 8
 variance 38
 velocity sensor 8, 12, 13, 23
 vibrations 17, 40
 winding mode 23